Journal of Thermal Analysis and Calorimetry (2025) 150:1907–1932
https://doi.org/10.1007/s10973-024-13873-3

Performance evaluation of various training functions using ANN to predict the thermal conductivity of EG/water-based GNP/CNC hybrid nanofluid for heat transfer application

Md. Munirul Hasan[1] · Md Mustafizur Rahman[2] · Suraya Abu Bakar[1] · Muhammad Nomani Kabir[3] · Devarajan Ramasamy[2] · A. H. M. Saifullah Sadi[4]

Received: 10 May 2024 / Accepted: 21 November 2024 / Published online: 10 January 2025

Abstract

Thermal management efficiency is still a significant problem in many industries and techniques due to the ultimate limitations in the performance of conventional heat transfer fluids. The present research focuses on predicting the thermophysical properties of hybrid graphene nanoplatelet (GNP) and cellulose nanocrystal (CNC) nanoparticles to improve the thermal performance of heat transfer systems. Resolving the thermal management issues can be critical for saving energy, enhancing the effectiveness of the systems, and advancing the existing and emerging technologies needed to handle high temperatures. GNP-CNC/ethylene glycol–water hybrid nanofluids were prepared in volume concentrations from 0.01 to 0.2%. Thermal conductivity was measured from 30 to 80 °C, providing comprehensive data for analysis. The most important resolution was formulated at 0.1% volume concentration within a 60:40 volume ratio of ethylene glycol and water, with UV–Vis analysis showing absorption peaks in the highest order at 0.10% and 0.2% concentrations. Thermogravimetric analysis has shown an increase towards thermal resilience, with the mass decline beginning at 130 °C and full degradation at 500 °C. An interesting observation was invested for 0.20% GNP: CNC, where the onset of degradation occurred at 150 °C, providing an increased variety of potential high temperatures. An artificial neural network (ANN) model was implemented to predict thermal conductivity, and 15 training functions were examined for the ANN structure. The model's best prediction results were obtained by utilizing tansig and Purlin transfer functions in a single hidden layer with ten neurons, which employed the Bayesian regularization function. It reached $R^2 = 99.99\%$, $\mathrm{MSE} = 4.8352 \times 10^{-7}$, and $\mathrm{RMSE} = 1.2083 \times 10^{-3}$, which is superior to other functions, e.g. trainlm. The novelty is successfully synthesizing a stable GNP-CNC hybrid nanofluid with excellent thermophysical properties and establishing a highly accurate predictive model. The impact could be widespread in various industries, from better cooling to more efficient energy systems, and even the applicability of this effect in improving industrial processes.

Keywords Thermal conductivity · Training functions · Artificial neural network · BR · LM

Introduction

Thermal management paradigms have changed totally within the last decade, where conventional heat transfer fluids have been substituted with advanced colloidal suspensions, particularly hybrid nanofluids. The described shift is associated with the peculiar heat transfer and flow regime of hybrid nanofluids, which provide a range of benefits and opportunities for improving the thermal efficiency of different systems and devices, from microelectronic to large industrial applications [1, 2]. The introduction of advanced nanofluids in coolant systems has resulted in an unprecedented increase in heat transfer rates and enabled the reduction in dimensions

✉ Md Mustafizur Rahman
mustafizur@umpsa.edu.my

1 Faculty of Computing, University Malaysia Pahang Al-Sultan Abdullah, 26600 Pekan, Pahang, Malaysia

2 Faculty of Mechanical and Automotive Engineering Technology, University Malaysia Pahang Al-Sultan Abdullah, 26600 Pekan, Pahang, Malaysia

3 Department of Computer Science and Engineering, United International University, United City, Madani Avenue, Badda, Dhaka 1212, Bangladesh

4 Department of Computer Science and Engineering, Uttara University, Dhaka 1230, Bangladesh

and mass of heat exchange components, which is especially important for the development of compact and efficient thermal systems [3, 4]. Hybrid nanofluids, dispersing two or more different nanoparticles in a base fluid matrix, have emerged as a leading edge in ranging from nanofluid technology [5]. This multi-component nature allows for the synergistic optimization of thermophysical properties through a good selection of nanomaterial combinations [6, 7]. The literature has reported that by combining the most beneficial characteristics of each nanoparticle type while alleviating respective limitations of single-component systems, properly formulated hybrid nanofluids could deliver up to 30–40% increases in thermal conductivity over conventional fluids [8]. Hybrid nanofluids potentially deliver better thermophysical properties for heat transfer applications in play with some other thermophysical properties such as viscosity, thermal conductivity, density, and shear rate [9, 10]. Among them, thermal conductivity can be identified as a vital governor of fluid heat transfer [11]. However, a complex interplay of parameters such as nanoparticle concentration in the base fluid, thermal conductivity enhancement temperature dependence, particle shape factor, wide size distribution, and specific surface area limits the predictability and optimization of hybrid nanofluid properties [12, 13]. This complex behaviour can be quantitatively expressed as dimensionless numbers, the Nusselt, Prandtl, and Reynolds numbers to characterize the convective heat transfer performance of the fluid system.

In recent research, more attention has been paid to carbon-based nanoparticles (NPs), such as graphene nanoplatelets (GNPs) and cellulose nanocrystals (CNC), because of their excellent thermal performance and environmentally friendly forms [14]. Significantly larger than more recent single-layer graphene, GNPs allow greater surface area for heat dissipation and enjoy many of the properties of tightly packed graphitic carbon. They are usually both strong and stable [15]. On the other hand, CNC is a nontoxic and biocompatible nanomaterial with a fibrillar structure (generally 5 nm in diameter), which leads it to be biodegradable and renewable, being an alternative to sustainable solutions for thermal management as well [16, 17]. Given their superior thermal properties and biodegradability, investigations have also been concerned about carbon-based NPs like graphene nanoplatelets or cellulose nanocrystals [17]. Recently, GNPs have attracted considerable attention, and significant progress has been made because of their relatively larger surface area, excellent thermal conductivity due to their multi-graphene layer constitution, and synergistic effects of densely packed graphitic carbon [18]. They are mechanically strong, chemically stable, and cheap [19]. They have very high aspect ratios, often exceeding 1000, allowing superior percolation networks in the fluid. In addition, wood (and hence Cellulose) is biodegradable, has an inherently renewable source, and is nontoxic and biocompatible [20], while CNC, by its fibrillar morphology (5–20 nm in diameter and 100–500 nm long), seems to be even less reactive [21, 22]. CNCs exhibit a relatively high thermal conductivity among organic materials, ranging from 0.5 to 1 $Wm^{-1}\ K^{-1}$, and possess unique rheological properties that can stabilize nanofluids and flow better in them [23]. The use of hybrid nanofluids combining GNPs and CNC can open up a window by which the high thermal conductivity of GNPs can be utilized along with the stabilizing and rheology-modifying characteristics of CNC.

The practice of adding GNPs and CNC in hybrid nanofluids has been found useful in automotive cooling. For instance, Yaw et al. [24] studied a hybrid nanofluid containing GNP and CNC nanoparticles dispersed in a mixture of water (W) and ethylene glycol (EG) (40:60). They showed that the results were considerably better than those obtained for the base fluid. There was an enhancement of 51.91% for the heat transfer coefficient at the lower side, of 46.72% related to the overall heat transfer coefficient in average values and pressure drop achieved up to 34.06%. The promoted heat transfer is due to thermal conductivity enhancement and flow behaviour modification, as described by the correlation for the Nusselt number in a turbulent flow. Similarly, Sandhya et al. [25] prepared GNP and hybrid GNP-CNC nanofluids in the water-EG carrier. The thermophysical properties were examined for heat transfer applications. The results reveal good thermal behaviour for both nanoparticles and superior thermal properties of the hybrid nanofluid compared to conventional water-based fluids, providing a potential alternative to an effective cooling solution for thermal management applications. Even though the result is quite interesting, the literature presents little work on GNPs/CNC hybrid nanofluids. These points highlight a gap in the literature that impedes an in-depth understanding of GNPs/CNC hybrid nanofluids and limits our ability to gauge their thermophysical performance, dispersion stability over long duration, and their prospect in advanced heat transfer energy systems [26]. Composite nanofluids are even more complex and require sophisticated modelling to predict and customize these properties accurately.

Artificial neural networks (ANN) are a powerful tool for analysing and forecasting thermophysical features because of their favourable performance properties, as reported in these works [27, 28]. ANN has excellent merits in analysing data, recognizing patterns, and modelling where researchers are able to identify complex relationships among different variables of nanofluids that might have been impossible in a mere correlation or regression equations from conventional statistics [29]. They recently reported that ANN applications predict thermal conductivity and viscosity in nanofluid compositions within different temperature ranges and concentrations. For example, Li et al. [30] conducted a thorough

study on the thermal conductivity, stability, and viscosity of an Al_2O_3/EG nanofluid. An ANN modelling was used across a 25–60 °C temperature range and 0–2% volume concentrations. ANN model was proved to be highly accurate where coefficients of determination (R^2) were 0.9997 and 0.9984 for thermal conductivity and viscosity, respectively, demonstrating the effectiveness of this model in predicting such fundamental properties of nanofluids. Rostami et al. [31] developed an ANN model to predict the thermal conductivity of MWCNTs-CuO/water hybrid nanofluid, and it has been proved that when the number of neutrons in the hidden layer is eight, the prediction results not only have high accuracy but also approach measurement results closely as well. At the same time, Esfe et al. [32] demonstrated ANN's ability to model the thermal conductivity of TiO_2/EG-H_2O nanofluids. In addition, Alizadeh et al. [33] tested ANN in predicting thermal conductivity for ZnO–TiO_2/EG hybrid nanofluid and showed that ANN has a more accurate forecasting ability than traditional fitting approaches. Overall, the results of all studies indicate that the ANN demonstrates strong performance in characterizing the thermal properties of various nanofluid compositions, confirming its potential as a promising tool in the context of nanofluid research and development. The results of all these studies demonstrate that the ANN can highly qualify for characterizing different nanofluids corresponding to their thermal properties, such potential behaviour having a bright future in nanofluid research and development. They further claim that the ANNs are always better when compared to traditional fitting techniques and have > 2% prediction errors. Tian et al. [34] used ANN modelling to check the effects of temperature and volume fraction on thermal conductivity with hybrid nanofluid graphene oxide-Al_2O_3/W-EG. The application of the ANN model trained by trainbr (correlation coefficient = 0.999, mean squared error = 1.67×10^{-6}) primarily affected the prediction of thermal conductivities. Moreover, Esfe et al. [35] demonstrate that Bayesian Regularization (BR) is exceptionally effective in predicting thermal conductivities of TiO_2/water nanofluids, achieving $R^2 = 99.9\%$ and MSE = 1.0211×10^{-5} using a 2–5–5–1 ANN architecture. One of the critical points in the effectiveness of ANN models is the optimization of their architecture and that of training algorithms. Recent works on the subject used a BR training algorithm, yielding rather good results [36, 37]. The approach minimizes a combination of squared errors of two varieties and masses. It creates a network that possesses better generalization properties. However, since the effectiveness of ANN models is limited by the quality of data they are exposed to, not all architectures are equally suitable for specific formulations. As a result, a wide range of architectures and various training functions have to be evaluated to determine the most optimal version of the ANN for each new type of hybrid nanofluid [38, 39].

The study proposed herein covers some critical research gaps in GNPs/CNC hybrid nanofluids, which enable better use in thermal management applications. The research encompasses a systematic synthesis and characterization of these nanofluids, targeting optimized thermal conductivity for improved heat transfer purposes. A critical aspect of the study is developing and optimizing an ANN model designed to accurately predict the thermal conductivity of GNPs/CNC hybrid nanofluids. The temperature and volume concentration are input parameters, ranging from 20 to 80 °C and 0.01 to 1%, respectively, with the specific synergistic effects between GNPs and CNC in mind. Various ANN architectures and training algorithms are compared to determine how to model the nanofluids best. At the same time, particular focus was also directed at researching the potential of the BR algorithm to enhance the accuracy of predictions and generalization of the model. It was possible to perform the sensitivity analysis, allowing us to determine which of the two parameters, temperature or concentration, is more critical for the changes in thermal conductivity. Moreover, the relative significance of the two quantified as well, which is of the utmost value when determining the main factors that govern the behaviour of GNPs/CNC hybrid nanofluids. A sensitivity analysis is also enabled to evaluate the relative impact of temperature and concentration on thermal conductivity. This can provide essential insights into the leading factors guiding the behaviour of GNPs/CNC hybrid nanofluids. The study aims to ensure superior understanding and prediction capabilities for GNPs/CNC hybrid nanofluids.

This paper aims to fill the gap between the experimental characterization and theoretical modelling of GNPs/CNC hybrid nanofluids by achieving the stated objectives. The creation of improved ANN models not only advances the understanding of these complex fluids but can also be used by engineers and developers to design and optimize advanced thermal management systems. Additionally, the results and findings of this research work are foreseen to provide added value in current technologies on nanofluids as well as drive advancements towards increasing applications of hybrid nanofluids within industrial and other sectors by integrating ease with enhancing effectiveness while bringing down their environmental impacts through enabling bridge between nature-friendly design schemes paving way onto high performance next-generation multi-functional thermal management materials.

Methods and materials

Experimental details

The experimental protocol employs a base fluid of W and EG along with a hybrid nanofluid system based on GNPs

Table 1 Thermophysical features of nanoparticles [25]

Properties	CNC	GNP
Purity	–	99.9%
Colour	White (dry powder)	Black
Structure	Crystalline form	Platelet shaped sheets
Density/kg m^{-3}	1050	2267
Specific surface area/ m^2 g^{-1}	–	800

Table 2 Thermophysical properties of base fluid [25]

Properties	EG ($C_2H_6O_2$)	Water
Vapour pressure/kPa	0.007	3.169
Density/kg m^{-3}	1100	1000
Viscosity/mPa s	16.59	1.0015
Molar mass/g mol^{-1}	62.07	18.0153
Specific heat/J kg^{-1} K^{-1}	2348	4178
Thermal conductivity/Wm^{-1} K^{-1}	0.258	0.608

and CNCs. After the preparation of this nanofluid, a complete analysis is carried out to evaluate stability and long-life dispersion. The GNPs used in this work have outstanding properties, like having a high specific surface area of 800 m^2 g^{-1}, enhancing their thermal and electrical conductivities. The purity of these nanoparticles is 99.9%, and the diameter varies from 1.5 nm to a thickness of only about 3 nm, which makes it one-dimensional and, therefore, possesses a high aspect ratio, promising substantial enhancements in base fluids properties due to nanoparticle addition.

The CNC nanoparticles possess different morphological and structural characteristics, as was discussed in the previous section. It shows an 80% crystallinity index, representing a high degree of structural ordering. The CNCs have a crystal diameter of 9 ~ 14 nm and a hydrodynamic diameter of 150 nm. The length of these nanoparticles ranges between 100 and 150 nm crystal-wise, which also contributes to inertia in reinforcing the nanofluid system. Table 1 provides detailed physical specifications of the nanoparticles (GNPs and CNCs) for a thorough examination. In addition, Table 2 presents critical properties related to density thermal conductivity and specific heat of two essential liquid components (water, ethylene glycol) in reference temperature equal to 20 °C, which can be used as essential factors based on considering research materials for this study.

Preparation of hybrid nanofluids

GNP-CNC/water-EG-based hybrid nanofluid was prepared using a standardized two-step method at the Advanced Automotive Liquid Laboratory (A2LL), Faculty of Mechanical and Automotive Engineering Technology, Universiti Malaysia Pahang Al-Sultan Abdullah. The schematic representation of the preparation of the hybrid nanofluid employs a flow diagram in Fig. 1. In this experiment, the 60% aqueous EG solution-based fluid which has a base composition of EG/W = 60:40 was used. The GNP-CNC hybrid nanofluids were synthesized at a 1:1 ratio of GNP and CNC, with volume concentrations ranging from 0.01 to 0.2%. Concentrations were given in four doses: 0.01%, 0.05%, 0.1%, and 0.2%. This process included dispersing the hybrid nanofluid into the base fluid using a magnetic stirrer at 400–500 rpm for 120–180 min. The stirring direction was reversed every 15 min to ensure uniform mixing. After the first dispersion, ultrasonication was performed to improve stability once without a surfactant. The process used a probe-type ultrasonic bath, which ran for 5 h at 50% power. The extended period of ultrasonication was necessary to ensure complete nanoparticle breakdown and uniform distribution throughout the base fluid. In order to give the fluid time to stabilize and reset, a 5 min off, for every 15 min, was used while sonication was taking place in an effort of properties with particle formation [40].

Stability analysis of the prepared nanofluids was necessary for possible practical applications. A sample was chosen based on its long-term stability properties. The process started by setting the optimum value for concentration and the needed ratio between GNP and CNC to be mixed with the base fluid well before starting their preparation. The nanoparticle dispersion in these base fluids was further characterized by surface analysis using scanning electron microscopy (SEM). This enabled capturing images at high resolutions of the distribution of CNC and graphene particles for different magnifications, as shown in Fig. 2. The quantifiable characteristics of the hybrid nanoparticles, such as mass, density, and volume concentration, were determined according to several well-known equations (Eqs. 1, 2, and 3) [41, 42]. These calculations provided essential information to characterize the produced nanofluids for further applications.

$$M_{\mathrm{CNC/GNP}} = \left(\frac{\phi}{100-\phi}\right) \times \left(\frac{\sigma(\mathrm{CNC/GNP})}{\sigma_{\mathrm{bf}}}\right) M_{\mathrm{bf}} \tag{1}$$

$$\sigma_{\mathrm{CNC/GNP}} = \frac{\sigma_{\mathrm{CNC}}\phi_{\mathrm{CNC}} + \sigma_{\mathrm{GNP}}\phi_{\mathrm{GNP}}}{\phi_{\mathrm{total}}} \tag{2}$$

$$\phi_{\mathrm{CNC/GNP}} = \frac{M_{\mathrm{CNC/GNP}}/\sigma_{\mathrm{bf}}}{M_{\mathrm{CNC/GNP}}/\sigma_{\mathrm{bf}} + M_{\mathrm{bf}}/\sigma(bf)} \tag{3}$$

where ϕ is the volume concentration of nanofluids, M is the mass, and σ is the density of the hybrid nanofluid. The subscripts GNP and CNC are nanoparticles, and *bf* denotes the base fluid.$M_{\mathrm{CNC/GNP}}$, $\sigma_{\mathrm{CNC/GNP}}$, and $\phi_{\mathrm{CNC/GNP}}$ are the

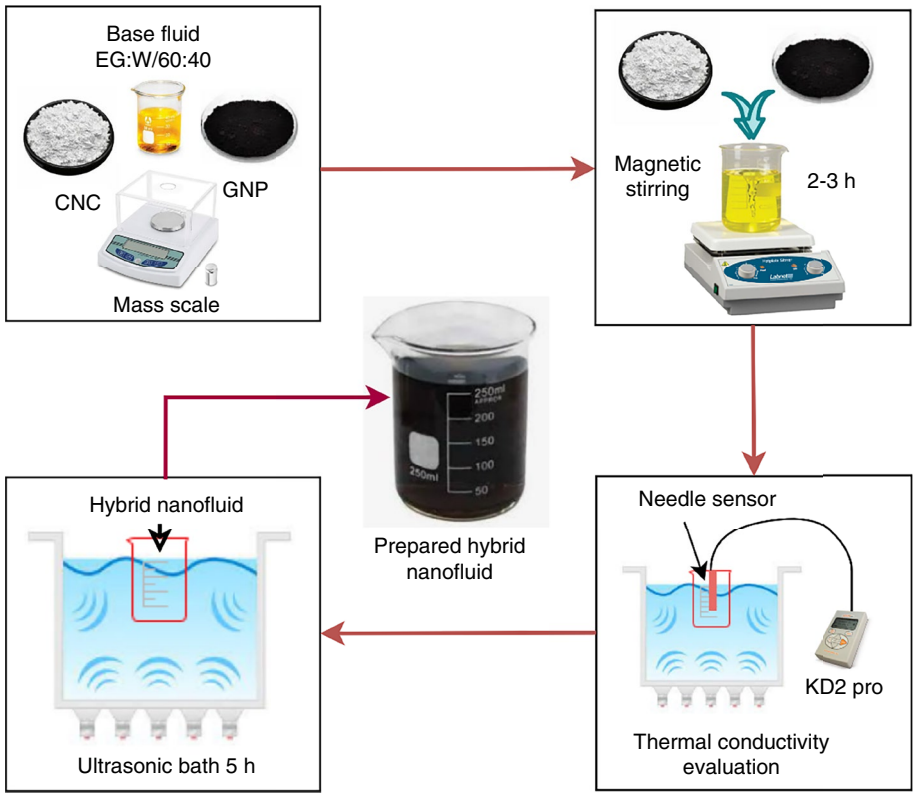

Fig. 1 Preparation of CNC/GNP hybrid nanofluid

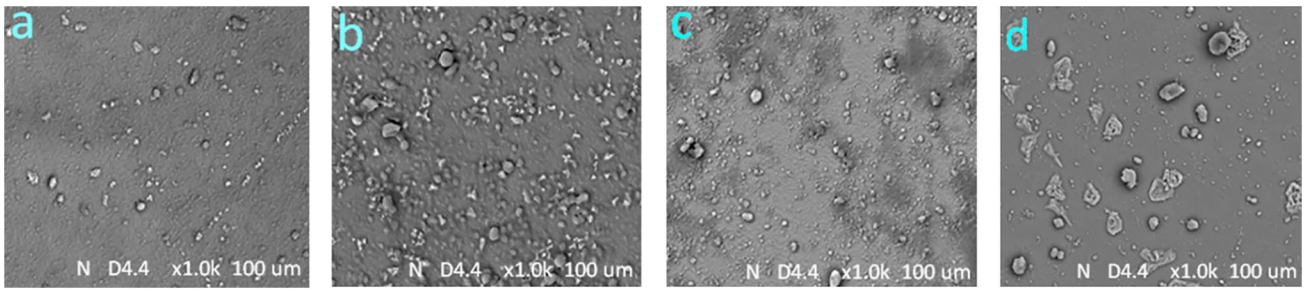

Fig. 2 SEM pictures of hybrid nanoparticles in the foundation fluid at various volume concentrations **a** 0.01 **b** 0.05 **c** 0.1 **d** 0.2

mass, density and volume concentration of the GNP and CNC nanoparticles. M_{bf} and σ_{bf} are the mass and density of the base fluid.

Stability analysis

Nanoparticles, characterized by their extensive surface area, tend to agglomerate, which poses a significant challenge to the stability of hybrid nanofluids. This stability is a critical factor in their practical application [43, 44]. To address this concern, a comprehensive investigation was conducted to assess the dispersibility and stability of nanofluids incorporating CNC: GNP nanoparticles. The assessment utilized multiple analytical methods to evaluate nanofluid stability. The sedimentation method, which included capturing images at various intervals, was employed to track particle settling visually. Zeta potential analysis was performed using a Zeta potential Anton Paar lite sizer 500 to quantify the repulsive forces between closely charged particles in the nanofluid dispersion. This measurement provides crucial insights into the stability of the colloidal system.

UV–Vis spectroscopy readings were obtained with a PerkinElmer LAMBDATM UV/Vis instrument (200–800 nm range). All samples were measured in specialized quartz cuvettes suitable for light absorbance measurements. The samples were diluted in the base fluid, after which spectra were taken to ensure satisfactory light scattering. Thermogravimetric Analysis (TGA): TGA was used to

examine the thermal stability of all prepared nanofluids. A TA device was used to perform this analysis under nitrogen. TGA was conducted in the 30–500 °C temperature range at a constant heat rate of 10 °C/min. This method gives an idea about the thermal decomposition behaviour of high temperatures of nanofluids and their stability. The results of the techniques used collectively offer an overall assessment of the dispersibility, colloidal stability, and thermal stability of CNC: GNP-based nanoparticle nanofluids, which makes them essential for their practical applications.

Visual observation

Due to the inherent hydrophobic property of GNP, their dispersion into base fluids is a challenge, as reported in previous studies [45]. This hydrophobicity results in GNP-repelling water (inherited from the CTAB coating), making it challenging to distribute within the fluid medium homogeneously. This issue is addressed by performing a systematic deposition process involved in nanofluid formation using ultrasonication homogenized GNP particles.

The stability post-preparation analysis was performed based on long-term visual preparation observation. As a result, the nanofluids based on GNPs showed outstanding stability, with no visible sedimentation detected over two months of storage before testing. Long-term stability is essential in applications, keeping the same thermophysical properties for a long time. Figure 3 shows the visual nanofluid stability at (a) as prepared, (b) 15 days and (c) 30 days after preparation. The photographs show how similar the nanofluid looks at these two seconds time points (Fig. 3a). At the 15-day mark (Fig. 3b), the absence of any visible sedimentation or phase separation indicates that the dispersion method worked well. This stability remained unchanged at day 30 (Fig. 3c), suggesting colloidal solid stability and resistance against long-term aggregation.

Analysis of UV–VIS spectroscopic

This research uses UV–vis spectroscopy to investigate the sedimentation behaviour of CNC and GNP nanoparticles. The study focuses on varying volume concentrations of these nanoparticles in EG/W mixtures, with spectral measurements conducted within the 200–800 nm wavelength range. UV-compatible quartz cuvettes were employed to measure the light absorbance of each sample at specific time intervals. The UV–vis spectrum analysis encompasses various dispersed, non-covalently modified GNPs and CNC nanoparticles. As illustrated in Fig. 4, all samples exhibit peak absorption within the 250–270 nm wavelength range. Following this peak, a consistent decrease in absorbance was

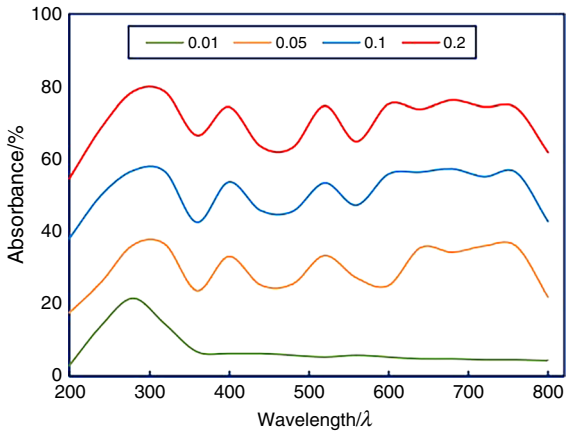

Fig. 4 Analysis of GNPs/CNC nanofluids using UV–Vis spectroscopy

Fig. 3 Stability test **a** after preparation, **b** after 15 days, and **c** after 30 days

observed across all tests within the same wavelength range, attributable to the presence of GNPs in all samples.

Notably, nanofluids with CNC: GNP volume concentrations of 0.01%, 0.05%, 0.10%, and 0.2% displayed distinct, wide absorbance bands. Furthermore, increased GNP: CNC concentration corresponded to widening the exposed band position for all samples. The UV–vis spectra indicate that the 0.20% GNP: CNC with EG/W nanofluid exhibited the highest absorption peak, suggesting superior nanofluid suspension stability among all tested concentrations. This comprehensive spectroscopic analysis provides valuable insights into the sedimentation behaviour and stability of CNC: GNP nanoparticles in EG/W mixtures, contributing to understanding these advanced nanomaterials and their potential applications.

Analysis of zeta potential

Zeta potential is an important factor for evaluating the stability of nanoparticle suspensions; it measures electrostatic repulsive and attractive forces between suspended particles [46]. The higher the absolute values of zeta potential, the better the stability, and being close to 0 mV means more aggregation. Generally, dispersions with zeta potentials above or below ± 30 mV are considered stable. In this study, stability analysis of hybrid nanofluids was conducted using the Anton Paar Litesizer 500 (Germany) to measure nanoparticle conductivity, which quantifies the potential difference across solid–liquid-phase boundaries. This method, also known as the Z-potential method, is widely recognized for evaluating colloidal suspension stability.

Figure 5 presents the zeta potential measurements, characterizing the colloidal stability of GNPs and CNC particles in EG-W base fluids. Zeta potential represents the particle charge at the shear plane, providing insights into particle interactions within the suspension. The electrical potential at the sliding plane, which separates mobile fluid from fluid adhered to the particle surface, is a key factor in this analysis [47]. In colloidal dispersions, zeta potential is synonymous with electrokinetic potential [48]. The experimental results (Fig. 5) show notably high zeta potential values, ranging from -69 to 79 mV. These values exceed the typical stability threshold of ± 30 mV, indicating strong electrostatic repulsion and, consequently, high dispersion stability.

The hybrid nanofluids exhibited the highest zeta potential magnitudes, with maximum values of 68.154 mV and 69.219 mV at 0.05% and 0.1% volume concentrations, respectively. The graphene dispersion demonstrated positive and negative zeta potentials, further confirming the high stability of these colloidal solutions. It is important to note that particles with positive zeta potential carry a positive charge, and colloids with high absolute zeta potential values (both positive and negative) are electrically stable. Conversely, colloids with low zeta potential are more prone to flocculation or coagulation [49]. The stability of colloidal dispersions is closely linked to the magnitude of their zeta potential. Particles with zeta potentials ranging from − 30 to+ 30 mV are generally considered stable due to sufficient electrostatic repulsion [50]. Furthermore, colloids exhibiting high absolute zeta potential values, whether positive or negative, demonstrate enhanced electrical stability. In contrast, systems with low zeta potential values are more prone to flocculation or coagulation, leading to reduced stability and potential sedimentation of particles.

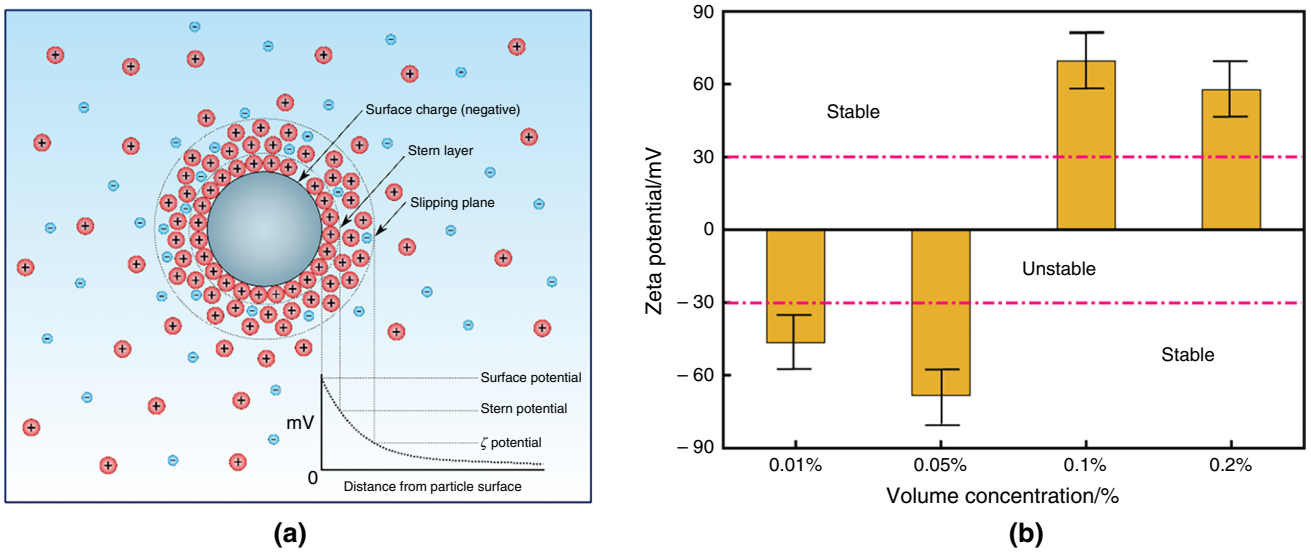

Fig. 5 **a** Diagram of zeta potential [42], **b** analysis of zeta potential of hybrid GNPs/CNC nanofluids

Measurement of thermal conductivity

Several methodologies have been presented to determine the effective thermal conductivity of nanofluids. The transient hot wire (THW) method is the most appropriate and fastest. A KD2-Pro hot wire test system (Decagon Devices Inc., USA) was used to measure the thermal conductivity of a W/EG-based GNPs/CNC hybrid nanofluid. The thermal conductivity of prepared hybrid nanofluid at different volume concentrations and temperatures is shown in Fig. 1.

A temperature bath (WNB7-MEMMERT, Germany) was used to achieve the accuracy of the control in measuring thermal conductivity. The need to minimize experimental errors requires careful handling of probe vibration. A horizontal frame was mounted on the given temperature bathtub, and the KS-1 probe was brought into a vertical position at the centre of the sample vial. Repeated 20 times for each volume concentration and temperature, there was a time of no less than 5 min between two measurements to assess data repeatability. The KD2-Pro thermal conductivity measurement probe has a particular set of specifications listed in Table 3.

Artificial neural network

Artificial neural network (ANN) is a computational model inspired by the structure and functions of biological neural networks in our human brain. It is made of interconnected nodes (like neurons) forming into layers. The input layer receives the original data; one or more hidden layers manipulate this information via massed connections. The only thing between itself and the model output is an activation function. This architecture reflects the parts of a biological neuron: dendrites to receive input (input nodes), the soma for processing signals (hidden layer nodes), and the axon that relays signals to other neurons (output node). In fact, in light of the success of deep learning and its recent increase in attention and wide applications across diverse machine learning tasks, this kind of biomimetic way is developed by ANNs to process complex data patterns efficiently (illustrated in Fig. 6) [43]. ANN can present computer modelling of experimental data more quickly than the mathematical model. The advantages of ANN include its simplicity, capacity to extract nonlinear relationships from training data, and capability to model multivariate issues for solving complex relationships between variables [44]. ANNs are favoured in many applications due to their distinctive capabilities over traditional machine learning methods. Particularly for smaller datasets, ANNs often outperform other machine learning models, making them a better choice in such scenarios [45].

Equation (4) represents the mathematical formula of an ANN network, where P_{ij} is the output of i neurons in the j layer, and f_j is the activation function, which can be tangent sigmoid, binary sigmoid, Gaussian, identity function, linear function, or any other. W_{ji} is the connected mass of every variable in i neuron in the j layer, selected randomly at the beginning of the training process. Z_j is the input vector, and b_{ij} is the bias of the i neuron in the j layer [46].

$$P_{ij} = f_j\left(\sum_{i=1}^{n} W_{ji}Z_j + b_{ij}\right) \tag{4}$$

There are various types of ANN models, and the training function is one of the most essential hyperparameters for differentiating them. Algorithms used in the ANN training process are shown in Table 4 with features. These algorithms significantly impact the functions, formations, and topology of ANNs. Unique features of various ANN models focus on and strengthen a specific component of the human brain's abilities and characteristics. However, the fundamental variation between the training functions is based on how they modify the masses and biases at different stages of training.

In general, the role of the training functions in the overall framework of ANNs can be connected to mass and bias. Mass is an adjustable crucial parameter in ANN that is responsible for regulating, weakening, or enhancing neuron

Table 3 Device features for thermal conductivity measurement

Accuracy ± 5%	Thermal conductivity
Operation range	0–80 °C
Measurement range	0.02–2 Wm^{-1} K^{-1}
KS-1sensor	Needle diameter: 1.3 mm Needle length: 60 mm

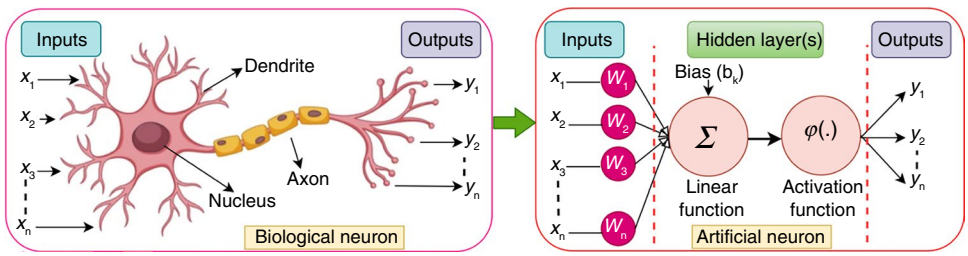

Fig. 6 Artificial neural network architecture from biological neurons [46]

Table 4 Features of training algorithms

Algorithms	Functions	Descriptions
Gradient descent Backpropagation (GD)	Traingd	In the traingd function, the masses and biases are obtained according to GD
Gradient Descent and Adaptive Learning Rate Backpropagation (GDA)	Traingda	In Traingda, the learning rate remains constant during the training and the masses, biases and adaptive learning rate are adjusted according to GD
Gradient Descent and Momentum (GDM)	Traingdm	In the Traingdm function in ANN momentum, masses and biases are investigated using Gradient descent
Momentum and Adaptive Learning Rate Backpropagation (GDX)	Traingdx	Traingdx training function updates the masses and biases according to gradient descent adaptive learning rate and momentum
One-Step Secant Backpropagation (OSS)	Trainoss	Trainoss function updates the masses and biases according to the one-step secant. Compared to the BFGS algorithm, it needs less computation and storage per epoch
Resilient Backpropagation (RP)	Trainrp	In ANN, the trainrp function is adapted to the masses and biases according to the behaviour of the error function. The size of the derivative does not affect the impact of the RP adaption system in contrast to other adaptive methods
Scaled Conjugate Gradient Backpropagation (SCG)	Trainscg	The masses and biases in the trainscg function are updated according to the SCG. This algorithm was proposed to eliminate the time-consuming line search, thus reducing the number of computation costs in each epoch
Polak-Ribi´ere Conjugate Gradient (CGP)	Traincgp	The masses and biases are adjusted in traincgp in ANN according to the conjugate gradient backpropagation of the Polak-Ribire update. However, the Polak-Ribiére needs slightly more storage than the Fletcher-Reeves
Fletcher-Reeves Conjugate Gradient (CGF)	Traincgf	In ANN, the traincgf function has adapted the masses and biases using Fletcher-Powell Conjugate Gradient
Powell/Beale Restarts Conjugate Gradient (CGB)	Traincgb	The masses and biases are evaluated in the traincgb function in ANN using conjugate gradient backpropagation with Powell-Beale restarts
Levenberg–Marquardt (LM)	Trainlm	Masses and biases are obtained in the trainlm function according to LM, and it requires more memory and computation cost due to the calculation of gradient and estimated Hessian matrix
Resilient Backpropagation (BR)	Ttrainbr	Masses and biases in the trainbr function are changed according to LM optimization. This function reduces squared errors and mass combinations and determines the appropriate combination to create a suitable ANN network
BFGS Quasi-Newton (BFG)	Trainbfg	According to BFGS Quasi-Newton, the masses and biases are obtained with the trainbfg function
Batch training (B)	Trainb	Trainb function trains a network with masses, biases and learning rules with batch updates. masses and biases are adjusted at the end of a complete pass by the input data
Cyclical order incremental (C)	Trainc	The trainc function trains a network with masses, biases and learning rules with incremental modifications after every presentation of an input
Random order incremental (R)	Trainr	masses and biases are changed following the Random order incremental

communication. The mathematical framework of the ANN model is the common denominator, which a set of parameters may modify. This control is responsible for the training process, and its objective is to obtain the proper output from ANN based on the needs and types of problems being investigated. In addition to the training procedure, the defined function in the ANN is a compelling case that plays a more familiar role in the formation structure [47].

Activation functions

In neural networks, activation functions are significant in learning abstract information via nonlinear transformations. It calculates the massed sum of inputs and biases and activates a neuron [48]. Thus, the number of neurons (s) in the hidden layer is defined by applying an activation function to find the desired output. The related coefficients in the hidden

layer are combined and grouped in matrices to generate a final output in the output layer [49]. Numerous activation functions exist in the literature. Some of them are presented in Table 5. Usually, a linear function (Purlin) is used to generate the final output of the ANN.

Evaluation metrics

The modelled and actual experimental data were compared using the coefficients and parameters calculation. Therefore, statistical metrics were used to calculate the correlation index and error measurement to assess the model fit. The regression coefficient (R) is broadly applied to infer the degree of linear correlation within the data. The mean square error (MSE) and root mean square error (RMSE) measure the quantity of the mean error in percentage terms [50, 51]. These metrics are calculated according to the mentioned equations:

$$R = 1 - \frac{\sum_{i=1}^{i=n}\left(X_{\exp(i)} - X_{\text{ann}(i)}\right)^2}{\sum_{i=1}^{i=n}\left(X_{\exp(i)} - X_{\text{ave}(i)}\right)^2} \tag{5}$$

$$MSE = \frac{1}{n}\sum_{i=1}^{i=n}\left(X_{\exp(i)} - X_{\text{ann}(i)}\right)^2 \tag{6}$$

$$RMSE = \sqrt{MSE} \tag{7}$$

$$MOD = \left(\frac{X_{\exp} - X_{\text{ann}}}{X_{\exp}}\right) \times 100 \tag{8}$$

where $X_{\exp}$ is the laboratory data, X_{ann} is the ANN output data, and n is the experiment number.

Suitable network configuration

Developing the optimal network with a suitable training algorithm is an important task, and it relies on numerous factors, for example, the complicacy of the problems, the volume of data in the training set, the number of masses, and bias in the network. As well as the error goal and network use for function approximation or pattern recognition are also essential factors in developing a suitable network [52]. In this study, various ANN models with multiple configurations were trained to determine an appropriate predictive model, and their outcomes were evaluated. Table 6 lists different training algorithms with their RMSE values and the number of neurons in the hidden layers. In this research, fifteen training algorithms were considered, while some training functions, either rarely used or not widely adopted, were excluded from the analysis. According to Table 6, using 36 datasets, the best result was achieved by the neural network with ten neurons in the hidden layer and the BR training algorithm. RMSE of this method was 5.9188×10^{-04}, the lowest error rate among the configured networks. Figure 7 shows the general structure of the optimized ANN configuration. This structure has one hidden layer, including ten neurons and an output layer. The most familiar transfer functions, tangent sigmoid (tansig) and purelin, are used for the hidden and output layers. Furthermore, to create an efficient ANN, 70% of the experimental data were utilized for training, 15% for the testing phase, and the residual 15% for the validation step.

Table 5 Features of activation functions [49]

Activation functions	Formula	Range	Features
Purlin	$f(x) = x$	$(-\infty, \infty)$	Differentiable, parametric, monotonic and smooth
Sigmoid	$f(x) = \frac{1}{1+e^{-x}}$	(0,1)	Differentiable, non-parametric, monotonic, smooth and bounded
Tanh	$f(x) = tantan(x) = \frac{(e^x - e^{-x})}{(e^x + e^{-x})}$	$(-1, 1)$	Differentiable, non-parametric, monotonic, non-smooth and bounded
ReLU	$f(x) = \begin{cases} xforx \geq 0 \\ 0forx < 0 \end{cases}$	$(0, \infty)$	Differentiable, non-parametric, monotonic, non-smooth and bounded for negative input only
LReLU	$f(x) = \begin{cases} xforx \geq 0 \\ 0.1xforx < 0 \end{cases}$	$(-\infty, \infty)$	Differentiable, non-parametric, monotonic, non-smooth and no-bounded
ELU	$f(a,x) = \begin{cases} xforx \geq 0 \\ a(e^x - 1)forx < 0 \end{cases}$	$(-1, \infty)$	Differentiable, parametric, monotonic, smooth and bounded for negative input only
Swish	$f(x) = x.sigmoid(x) = \frac{1}{1+e^{-x}}$	$(-\infty, \infty)$	Differentiable, parametric, non-monotonic, smooth and no-bounded
APL	$f(x) = (0,x) + \sum_{k=1}^{k} a_k \times \max(0, -x)$	$(-\infty, \infty)$	Differentiable, parametric, non-monotonic, non-smooth and no-bounded

Table 6 RMSE values of the existing training algorithms

Training functions	Network configurations					
	2–5–1	2–10–1	2–15–1	2–5–5–1	2–10–10–1	2–5–10–1
trainblm	0.00931	0.00392	0.06782	0.00617	0.00590	0.01378
trainbfg	0.01662	0.01960	0.02306	0.01988	0.01934	0.01910
trainscg	0.02285	0.23664	0.37788	0.01598	0.09591	0.11575
traincgf	0.03116	0.30099	0.64899	0.01838	0.03050	0.05477
trainoss	0.01524	0.73613	0.39522	0.02037	0.01841	0.01910
traingdm	0.64976	0.12767	1.37731	0.16583	0.14456	0.33630
trainbr	0.00268	0.00059	0.00589	0.00567	0.00853	0.00088
traincgb	0.01558	0.32680	0.25612	0.01273	0.09848	0.01703
traincgp	0.08485	0.31032	0.24515	0.01811	0.10392	0.01527
traingdx	0.24372	0.79126	0.60770	0.01262	0.15811	0.33630
traingd	0.04472	0.07071	1.37731	0.01755	0.26324	0.33630
trainr	0.02207	0.03162	0.04898	0.02523	0.03074	0.04242
trainrp	0.30983	0.27153	0.28982	0.07549	0.11180	0.01932
trainb	0.64976	0.12767	1.37731	0.16583	0.14456	0.33630
traibc	0.01267	0.01791	0.01900	0.02235	0.01025	0.01504

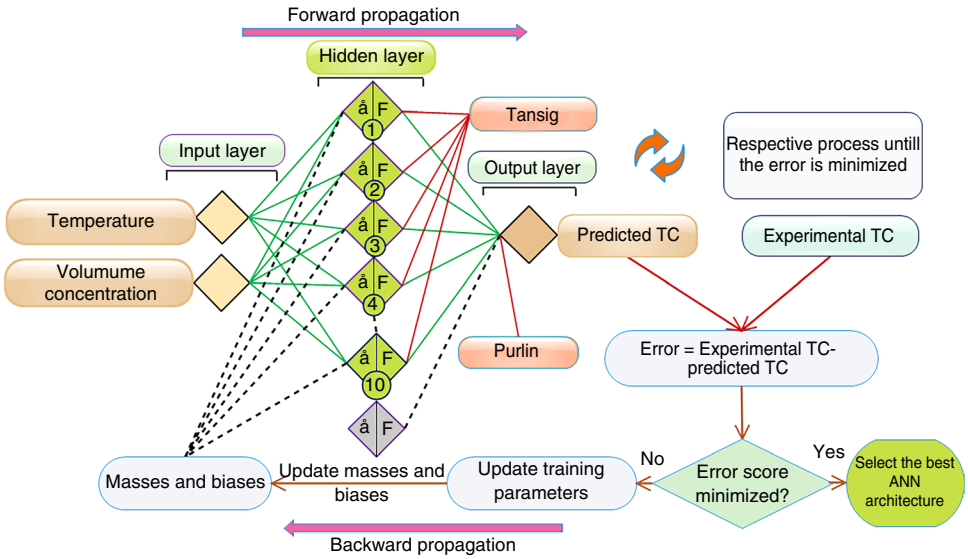

Fig. 7 Proposed ANN architecture

Results and discussion

Thermogravimetric analysis

Thermogravimetric analysis (TGA) of GNP: CNC-EG/W nanofluids with different volume concentrations gives essential information about thermal stability and degradation behaviour. As illustrated in Fig. 8, the TGA showed unique mass loss trends for various combinations of GNPs and CNCs, which suggests an intricate balance between nanoparticle composition and thermal behaviour. The GNP + CNC nanofluid (0.01–0.05%) has the first mass loss at about 130 °C, where this value corresponds to higher concentration levels of GNP + CNC composite < 100 nm particles and > 50% moisture evaporation [51]. The explanation of such an initial mass decrease can be ascribed mainly concerning some water present being lost [52], while for nanosize smaller than fly ash bare ceramic sample decomposition path shows only two significant thermogravimetry degradation peaks in different temperature regions being interaction among several remaining sites more likely by pyrolysis course exponentially over time due lower energy transitionary state consistent with collision theory [53]. This shift in degradation temperature with an increase in nanoparticle concentration is due to an improvement in the thermal stability of hybrid nanofluids.

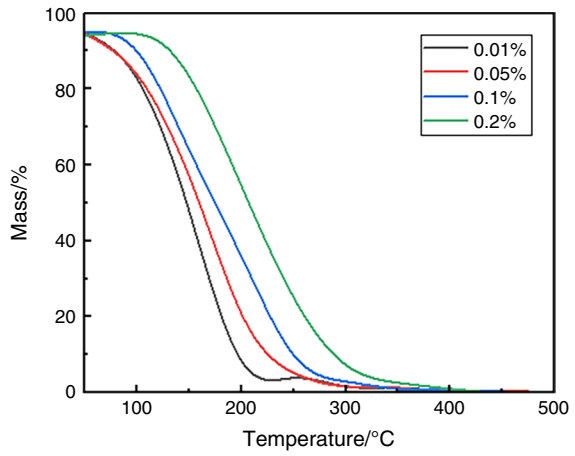

Fig. 8 Thermal decomposition behaviour presenting mass loss of the GNPs/CNC hybrid nanofluid as a function of temperature

The upward shift in the TGA curve with increasing GNP: CNC concentration shown in Fig. 8 indicates improved thermal resistance of the nanofluid compared to the base fluid (EG/W). Compared with functionalized graphene nanoplatelet-based nanofluids, this observation agrees with earlier research that indicated thermal stability enhancement [54]. The main mass loss at about 200 °C is generally attributed to eliminating surface oxygen-containing functional groups, as seen with most carbon-based nanomaterials [55]. Moreover, the mass variation in the atmosphere can be justified by a mixture of carbon oxidation to gaseous CO_2 and also metal catalysts remaining [2]. Therefore, the thermal characteristics of a hybrid nanofluid demonstrate considerable degradation behaviour and include many action mechanisms. The results of TGA provide important information about the thermal stability and degradation mechanism of GNP: CNC-EG/W nanofluids. It can be seen that this nanofluid is suitable for high-temperature applications. The fact that the rate of thermal degradation increases with increasing concentration of the nanoparticles implies that the hybrid nanofluid should be especially useful for advanced heat transfer systems operating at a higher temperature [56].

Thermal conductivity of CNC-GNPs

The thermal conductivity of GNPs and CNCs hybrid nanofluids was meticulously assessed with a temperature scope of 30–70 °C and volume densities of 0.01–0.2%. Figure 9 portrays the thermal conductivity variations as capacities of temperature and concentration. The hybrid nanofluids consistently demonstrated over sixty per cent greater thermal conductivity than pure ethylene glycol across all examined concentrations and temperatures. This enhancement can be attributed to incorporating nanoparticles that benefit from superior thermal attributes relative to the standard value established by ASHRAE for a forty per cent EG solution [57]. The expanding temperature expanded the warm movement of particles, bringing about higher conductivity. Moreover, expanding the nanoparticle focus expanded the pathways for heat dissemination. This brought about higher conductivity at higher temperatures and concentrations.

Furthermore, an increase in nanoparticle concentration at constant temperature considerably increases the thermal conductivity of the GNP/CNC hybrid nanofluid. The increase in thermal conductivity was explained by the enhancement of interfacial area between conducting nanoparticles and base fluid due to increasing nanoparticle volume fraction [58]. The increase in the interfacial region assists in improving thermal energy transmission across the solid–liquid interface, enhancing heat conduction capability for the nanofluid system. The positive temperature dependence of thermal conductivity is also exhibited, which can be explained by the enhanced Brownian motion with increasing temperatures [59, 60]. This extra thermal energy produces more violent collisions between nanoparticles and fluid molecules. The more interactions between particles, the higher the transfer of energy and, thus, the higher the thermal conductivity. This reveals a nonlinear characteristic of heat transfer in hybrid nanofluid systems, which includes the synergistic effect of nanoparticle amount and temperature on thermal conductivity.

The positive correlation between thermal conductivity and temperature can be explained by the intensification of Brownian motion at elevated temperatures, as corroborated by recent work from Asadi et al. [54]. Their study on MgO/MWCNT hybrid nanofluids demonstrated that increased particle movement results in more frequent collisions, generating additional kinetic energy and enhancing thermal conductivity. Figure 9a reveals a more pronounced temperature effect on thermal conductivity at higher volume concentrations, suggesting a synergistic interaction between temperature and concentration. To quantify the enhancement in thermal conductivity, Eq. (9) is employed:

$$\text{Thermal conductivity increment } (\%) = \left(\frac{\varphi_{\text{nf}}}{\varphi_{\text{bf}}} - 1\right) \times 100 \tag{9}$$

Figure 9c depicts the percentage enhancement in thermal conductivity across various concentrations and temperatures. The 0.01% concentration exhibited the lowest increase, while the 0.2% concentration demonstrated the maximum improvement, reaching 27.46% at 60 °C. The results confirm the promise of applying higher concentrations and temperatures of GNPs/CNC hybrid nanofluids for heat transfer applications. Such observed augmented thermal conductivity in these nanofluids is promising as they could significantly upgrade the traditional coolants in their applications for thermal management systems. Additionally,

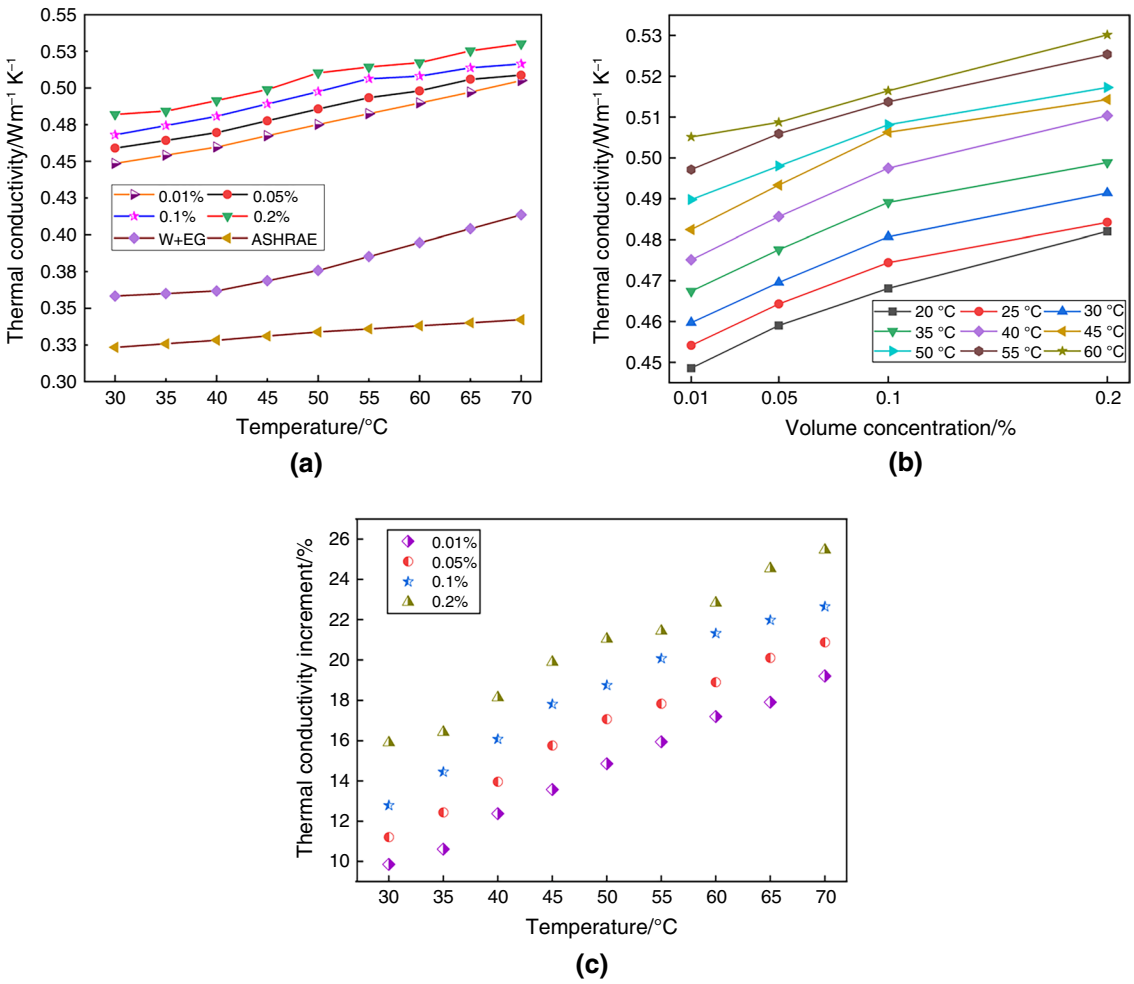

Fig. 9 Thermal conductivity at different **a** temperatures, **b** volume concentrations (**c**), and increment of thermal conductivity in percentage at different temperatures and concentrations

the synergetic effects reported from GNPs/CNC particles added to this argumentative statement that possibly hybrid nanofluids offer excellent cooling performance.

ANN analysis

Table 7 compares the performance of different training functions used in the ANN model to comprehensively predict thermal conductivity data for hybridized EG/W base with GNP/CNC hybrid nanofluid. Further, thermal conductivity is predicted as a target variable from the input parameters and temperature and volume fraction in ANN models. This comparison showed the ability to capture the thermophysical properties of nanofluids, with its inherent complex nonlinear relationships. The BR algorithm performs best; the lowest MSE values are 4.8352×10^{-7} and 8.8993×10^{-6} for training and testing sets, correspondingly, at 491 epoch. Levenberg–Marquardt (LM) presents relatively high efficiency: 9.0807×10^{-6} and 5.4869×10^{-5} for training and testing sets. Other training functions have MSE values from 10^{-4} to 10^{-5}. The distribution of errors in the entire dataset is from 10^{-7} to 10^{-1}. Notably, the gradient descent with an adaptive learning rate exhibits the highest error equal to 6.261×10^{-1}, evidence of relatively low effectiveness. For the same reason, the BR algorithm demonstrates the lowest error: 1.6431×10^{-6}. The results for the remaining algorithms may be characterized as relatively moderate, and the performance is expected in most cases. At the same time, the LM always performs better than the remaining algorithms, but it is still not as accurate as BR. As for the time for computations, this factor is almost the same for both backpropagation methods apart from only one exception, implementation for the conjugate gradient backpropagation with Fletcher-Reeves updates. The results of the BR algorithm show the best performance with the minimum value of the margin of deviation (MOD). This algorithm most effectively minimizes the deviation of predictions from the experimental

Table 7 Comparative performance analysis of ANN training algorithms for thermal conductivity prediction of EG/W-based GNP/CNC hybrid nanofluid

Training functions	Regression coefficients, *R*		MSE		MSE for all data	MOD, %	Gradient	Times	Epochs
	Train	Test	Train	Test					
trainlm	0.9991	0.9924	9.08×10^{-6}	5.48×10^{-5}	3.06×10^{-6}	1.12	4.45×10^{-5}	0.059	13
trainbr	0.9999	0.9991	4.83×10^{-7}	8.89×10^{-6}	1.46×10^{-6}	1.00	3.29×10^{-7}	0.059	491
trainbfg	0.9117	0.9936	3.86×10^{-4}	3.73×10^{-4}	2.51×10^{-4}	1.32	3.22×10^{-3}	0.059	26
trainscg	0.9350	0.9112	4.17×10^{-5}	1.02×10^{-4}	3.13×10^{-2}	1.58	2.52×10^{-1}	0.059	36
traincgf	0.9765	0.9901	1.52×10^{-5}	1.21×10^{-5}	7.24×10^{-2}	1.61	1.17	0.117	25
traincgp	0.9821	0.9899	1.16×10^{-5}	6.48×10^{-5}	6.90×10^{-2}	1.57	5.43×10^{-2}	0.059	19
traincgb	0.9865	0.9864	8.75×10^{-6}	1.01×10^{-5}	3.06×10^{-2}	1.47	2.15×10^{-2}	0.060	27
traingdm	0.4984	0.6164	2.10×10^{-3}	7.93×10^{-4}	1.23×10^{-2}	1.94	9.47×10^{-1}	0.059	30
traingdx	0.3908	0.7782	5.48×10^{-1}	1.40	6.26×10^{-1}	2.30	3.12	0.059	14
traingd	0.4167	0.5610	2.13×10^{-3}	7.94×10^{-4}	2.91×10^{-4}	1.86	7.60×10^{-3}	0.060	1000
trainoss	0.9241	0.9337	8.08×10^{-4}	8.11×10^{-4}	1.02×10^{-1}	1.79	3.22	0.059	8
trainr	0.4548	0.9813	5.91×10^{-4}	3.95×10^{-4}	8.22×10^{-4}	1.91	–	0.059	13
trainrp	0.8081	0.9209	1.79×10^{-4}	3.12×10^{-4}	3.36×10^{-2}	1.76	6.04×10^{-1}	0.059	27
trainb	0.4529	0.6522	6.15×10^{-4}	4.04×10^{-4}	1.23×10^{-2}	1.68	9.47×10^{-1}	0.059	6
trainc	0.8902	0.8908	7.07×10^{-5}	2.63×10^{-4}	2.56×10^{-4}	1.41	-	0.058	1000

data. The second-best algorithm is the LM algorithm, as its MOD is close to the BR's, which implies that it is more accurate in predictions.

The worst algorithm performance is gradient descent with adaptive learning rate (GDX), as the MOD is approximately 10.71265. These results illustrate which algorithms can make more accurate predictions, and this information resonates with the MSE analysis. It is noted that for the EG/W-based GNP/CNC hybrid nanofluid, the BR algorithm dominates all others, which the LM and other algorithms can follow hierarchically based on the accuracy for predicting the thermal conductivity. Results show essential performance differences in training the ANN to predict the thermal conductivity of EG/W-based GNP/CNC hybrid nanofluids, with the BR algorithm being the most accurate and reliable. BR's automatic regularization properties provide an optimum balance between model complexity and fit accuracy; the ability to fully exploit is important for nanofluid modelling where input parameters versus thermophysical property relationships are highly nonlinear [61]. The enhanced generalization of BR that results from its mass optimization being a probabilistic approach enables better prediction for properties of new unseen nanofluid compositions. Being the properties of nanofluids very sensitive to some slight changes in their composition [62]. The second-best player, the LM algorithm, performs well due to its unique optimization properties. However, its limited optimality characteristic has kept it relevant for problems with moderate complexities, such as in predicting the thermal conductivity of a nanofluid [21], because LM's efficient local optimization method results in both the stability from gradient descent and performance by Newton's method [63]. In addition, the inverse problems of nonlinear nature in LM could be purportedly solved to a good extent and correlated well with real-world nanofluids as sometimes even significant temperature- and concentration-dependent thermal conductivities are detected [64].

The variation in performance between different gradient-based methods and the poor results of simple gradient descent models is another effect made increasingly apparent by considering nanofluid property prediction an intricate optimization landscape. The thermal conductivity prediction is a non-convex optimization task, and it does not have only one global solution but numerous local solutions. In contrast, conjugate gradient methods (CGF, CGP, SCG) can traverse the error surface much better than standard gradients-based descent due to using some additional information during this traversing. This is because they harness the information from past evolutions to guide the search in the current direction [65]. The sensitivity mentioned above of simple gradient descent methods to initial conditions and learning rates is a particular problem in the area of nanofluid modelling; there may be orders-of-magnitude differences in scales between different input parameters, necessitating that poor-initial-guess solvers can converge. Our results are also consistent with the exhaustive comparison of gradient descent optimization algorithms, demonstrating poor performance for these methods in highly complex and multi-dimensional problems [66].

The potential impacts of these results on the modelling nanofluid property development are substantial. The high

predictability of BR indicates that ANNs can be used as efficient prediction tools for physical properties, namely the nanofluids characteristics, so a considerable reduction in experimental work can also be achieved. Bahiraei and Heshmatian [67] noted that current modelling techniques are inaccurate. As BR made the prediction in this time window and reached a high accuracy (compared to other algorithms), it is assumed that nanofluid-based systems can be simulated quickly with acceptable predictions crucial for real-time applications. Furthermore, even more accurate models for nanofluid property prediction could be developed by exploring hybrid algorithms that combine the strengths of BR and LM. In addition, transfer learning techniques may significantly accelerate the development of predictive models for nanofluid compositions that are new to the limited existing datasets [68]. Lastly, including physical constraints and the known behaviour of nanofluids in neural network architectures in line with the principles of physics-informed neural networks could significantly increase the accuracy and interpretability of predictions [69].

As illustrated in Fig. 10, BR performs slightly better than the other methods, with Bayesian Regularization and Levenberg–Marquardt dominating all training methods. The excellent performance of the BR algorithm, with near-one regression coefficients for training and testing sets, is attributed to its particular way of performing regularization. This new BR allows nonlinearity and decreases overfitting inherent in ANN modelling with complex systems [70]. Results The BR and LM learning rates outperformed other network training algorithms, with BR showing slight superiority. The BR and LM possess regression coefficient values near unity for training and testing datasets, indicating their remarkably high predictive accuracy. Still, BR consistently performs better than LM and has a slightly better generalization capability.

The significantly lower MSE and RMSE values by BR and LM, as observed in Fig. 10b, further support their better predictive performance compared to other considered models of our work. This improvement in accuracy is due to the new feature of these algorithms that handles the nonlinear nature of nanofluid composition, temperature, and thermal conductivity well. The complicated interaction of GNPs and CNCs with EG/W gives a nonlinear system that should be modelled by techniques like BR and LM rather than simple algorithms [71]. Other algorithms, especially the gradient descent-based ones, were poor performers due to the highly challenging nature of nanofluid thermal conductivity prediction. However, gradient descent-based algorithms are expected to be confused with local minima, especially for complex and non-convex error surfaces such as nanofluid systems [72]. There is superior performance of BR and LM. The role of sophisticated optimization methods in representing the intricate physics contained in nanofluids. In addition, it is essential to point out that the different nature of GNP/CNC hybrid nanofluid may also significantly affect the performance gap between algorithms. The unique synergistic effects between graphene nanoplatelets and cellulose nanocrystals create a complex thermal transport mechanism that demands sophisticated modelling approaches [73]. This better ability to capture these relationships by BR and LM compared to other algorithms in prediction property shows the importance of proper algorithm selection for nanofluid properties characterization. Figure 10b shows the MSE and RMSE values over both datasets and algorithms with a logarithmic scale on its y-axis, which is crucial to visualize the wide range of error values of different algorithms. This approach for visualizing the model performance differences in an extensive range of error magnitudes makes it easy to appreciate how much worse BR/LM is compared to other algorithms [74].

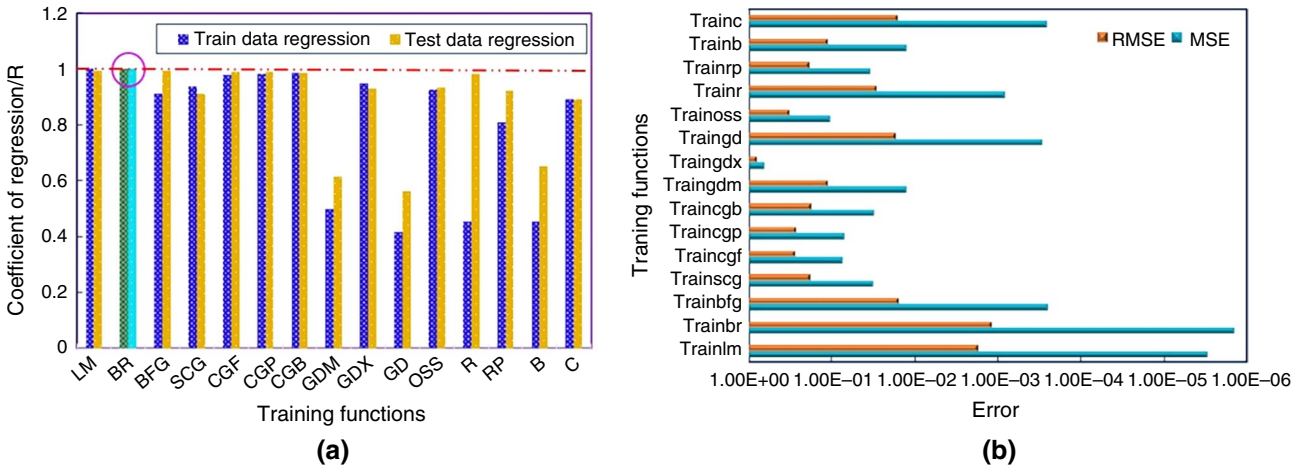

Fig. 10 Coefficient of regression for **a** training and testing data, **b** MSE and RMSE of various training functions

The performance curves of various training algorithms used for predicting the thermal conductivity of EG/W-based GNP-CNC hybrid nanofluids are presented in Fig. 11. As is visible from the plots, different approaches demonstrate varying tendencies to converge. In contrast, the optimal performance points are marked with circles, which means that the highest success in generalization is observed at these points before the onset of overfitting. The BR algorithm achieves a low error level and may be deemed the most successful approach since its deficient error equals 4.8352×10^{-7} at 491 epochs. The significant training period may pass while the stage of overfitting is not initiated, indicating the

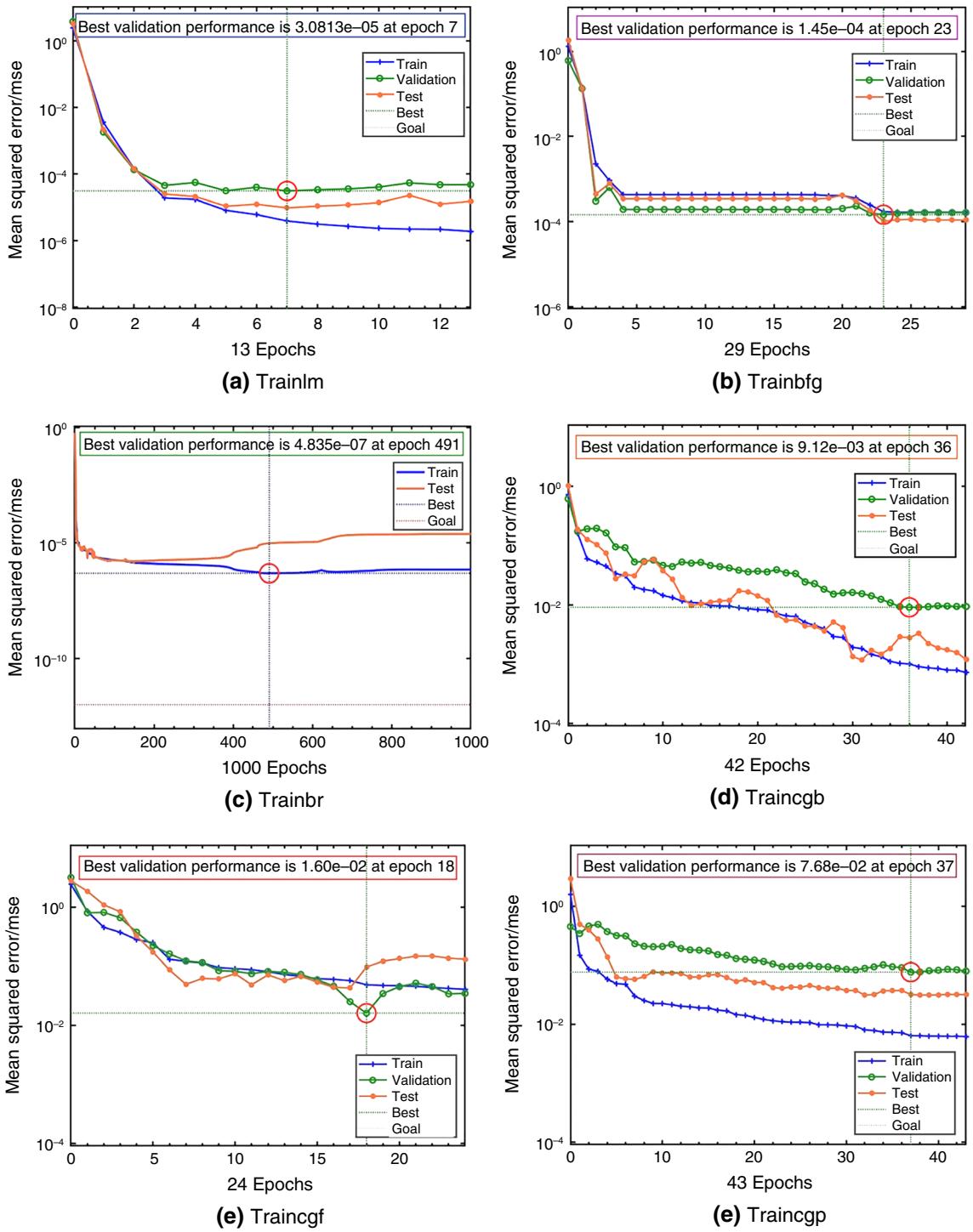

Fig. 11 Performance plot of different training functions

excellent generalization of BR, a feature enabled by the innovative mass regularization [70]. Meanwhile, the LM algorithm demonstrates the quickest convergence since its best validation performance is reached, and the error equals 3.0813×10^{-5} at only seven epochs. This tendency is typical for LM in moderately difficult problems [75].

The performance of other algorithms, such as BFG, CGB, CGF, and CGP, exhibits different convergence behaviours and error magnitudes. For example, BFG reaches 2.4526×10^{-4} at 29 epochs. Similarly, CGB, CGF, and CGP attain 9.1253×10^{-3}, 1.6083×10^{-2} and 7.6826×10^{-2} at 36, 18, and 37 epochs, respectively. This variation in performance could be attributed to the error surface each algorithm must move across, with each approach exhibiting a particular strength concerning this move with unique strengths in balancing convergence speed and accuracy [76]. Hence, BR and LM seemed to be much more effective in predicting the average convection in a nanofluid problem because it shows a degree of high nonlinearity. The interaction between GNPs and CNCs in the EG/W base fluid forms a highly nonlinear system [77]. Moreover, the variation in the optimal epoch numbers among several algorithms points to the significance of early stopping techniques for combating overfitting, which is critical in nanofluid property modelling (where the underlying physics is not fully understood). BR's ability to keep improving over many epochs without overfitting is a significant advantage in this field, letting the model pick up on delicate patterns that may have critical implications for accurate predictions.

The gradient values analysis over different training functions in Table 7 indicates useful information about ANN algorithms optimization behaviour for nanoparticle thermal conductivity prediction. While no algorithm was consistently the best performer, LM, BR, and BFGS were stable performers in each category but duplication, with BR as a clear choice for stability. This consistency in gradient values is essential for models to converge and demonstrates their robustness while traversing in the nonlinear parameter space of nanofluid systems [78]. The data presented in Fig. 12 in terms of the visualization of training state parameters and gradients for a few algorithms can support that the performance of BR is outstanding. The values of the gradients for the described algorithm are significantly better than those of other examples. The reason for such superior gradient behaviour is closely connected with the optimization approach of BR. It is mentioned that this method is unique because it minimizes training errors and regularizes the masses of a network [70]. As a result, this algorithm finds a perfect balance between fitting a training dataset and maintaining good generalization abilities [79].

The results revealing the high performance of BR in building the optimal neural network adequately mirror some of the recent studies' results about nanofluid property prediction. For example, Ahmadi et al. [75] reported that BR allowed for adequately modelling nanofluid viscosity, an effect that can also be related to the algorithm's ability to prevent overfitting in complex fluid systems. Because neural networks are built using a process that continually adjusts the citation masses and biases to minimize the combination of squared errors and masses that guide the evolution of the network, they have an advantage in terms of finding the complex combinations between particle characteristics, base fluid properties, and the resulting conductivity [80]. Even though LM and BFG have demonstrated relatively stable behaviour, the inferior performance of these methods compared to BR can be understood by considering that BR is able to estimate optimal regularization parameters intrinsically. This makes its ability a promising solution of BR to detect complexity and the specific issues that occur in hybrid system GNP/CNC nanofluid [36]. This is essential for nanofluids as often the underlying mechanisms governing their thermal conductivities are not fully understood, and even slight changes in nanoparticle composition can dramatically change the liquid convective heat transfer coefficient [77]. Hence, the generalization power of this form is significant. Hence, the performance of the BR algorithm on the fluid property prediction supports that it can be used for characterizing and predicting thermophysical properties in a nanofluid system, which is consistent with the recent trend towards implementing advanced data mining techniques [81]. The optimization method is consistent with the nature of nanofluid thermal conductivity prediction, which contributes to efficient BR algorithms flourishing and superior gradient behaviour.

Performance analysis at training, testing, and overall data stages demonstrates that the model developed is robust and accurate in capturing intricate relationships between nanofluid composition, temperature, and thermal conductivity. As shown in Fig. 13a, the model has reached an impressively low MSE of 2.6123×10^{-7} during training, suggesting it learns well and fits on data effectively with good generalization. This ultra-low error rate is possible thanks to the approach by which regularization in the BR algorithm is handled, where an innovative criterion of control over complexity and generalized performance succeeded [36]. Figure 13b–d extends the comparison, supporting our model's high predictive performance across training/testing/overall datasets. This agreement, combined with regression coefficients that consistently exceeded 0.999 for all datasets (Table 2), indicated the model's reliability and accuracy. This level of accuracy is particularly noteworthy given the complex nature of thermal conductivity in hybrid nanofluids, where synergistic effects between different nanoparticles (GNP and CNC in this case) and the base fluid (EG/W) create intricate heat transfer mechanisms [82]. The consistent high performance across all stages (training, testing, and

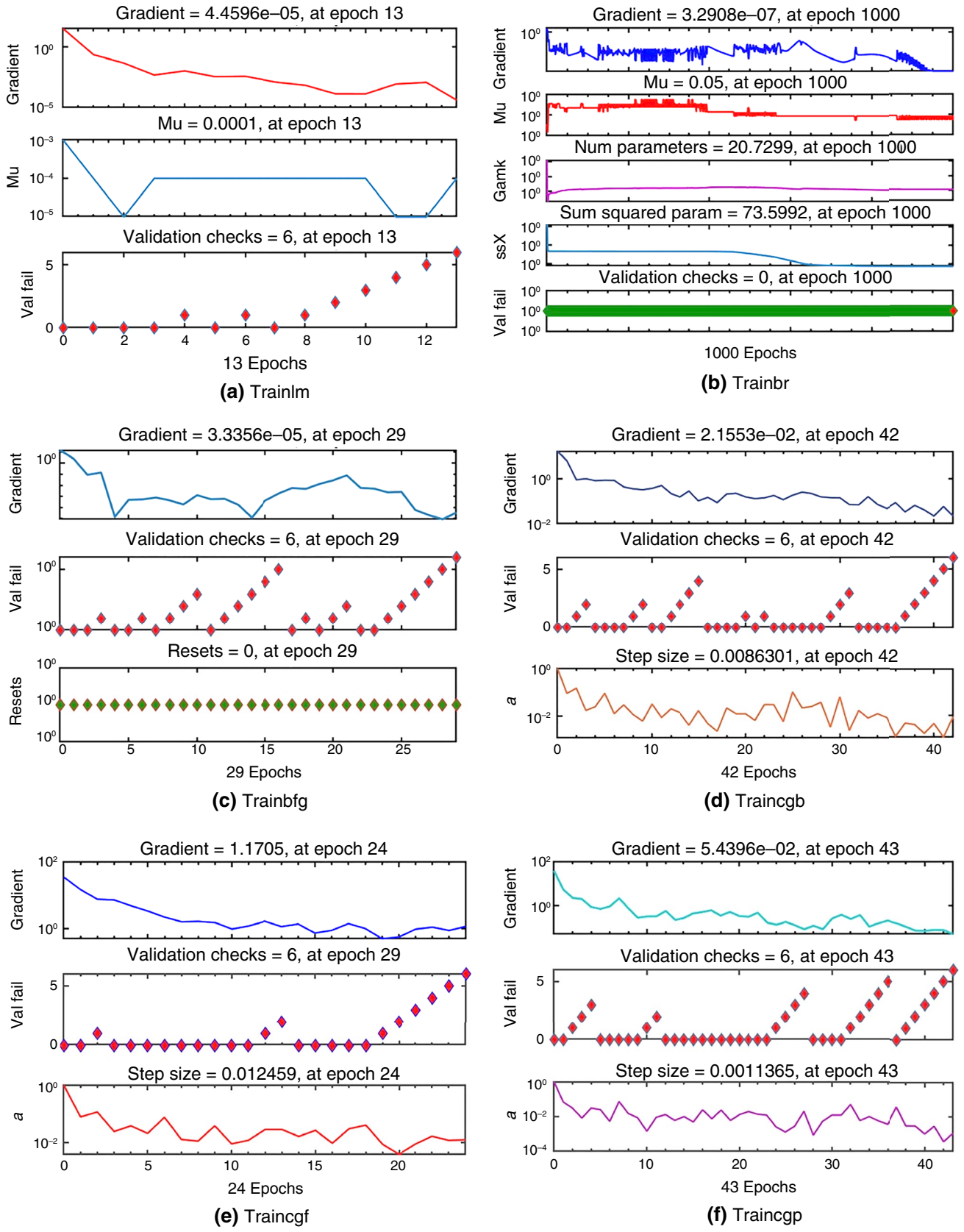

Fig. 12 Training state parameters of different training functions

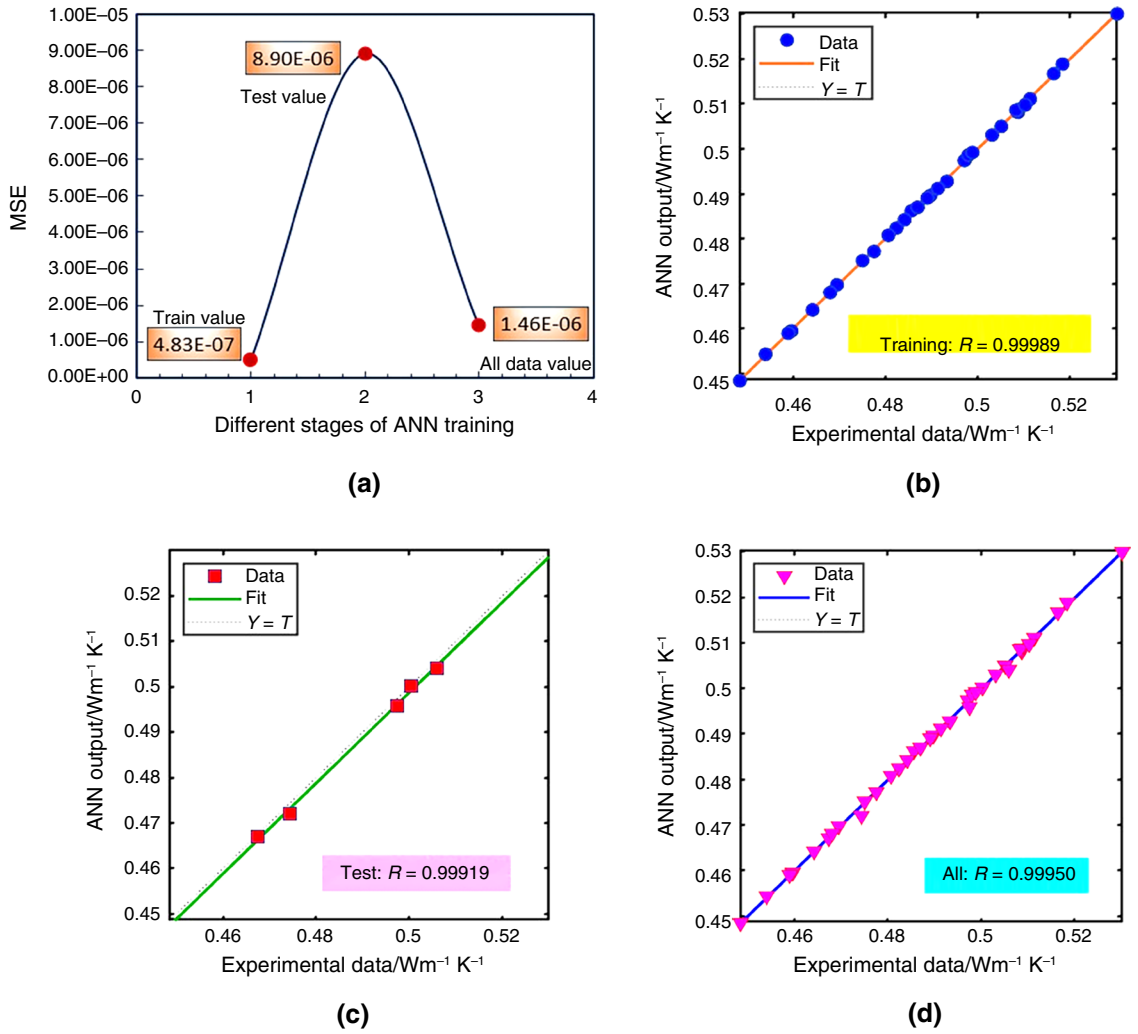

Fig. 13 **a** MSE values of different stages of ANN training. Regression graph of the ANN model for **a** training, **b** testing, and **c** all data set

overall data) indicates the model's robust generalization capabilities. This is a critical feature in nanofluid property prediction, where the underlying physical phenomena are often not fully understood or easily modelled using traditional methods [75, 83]. With findings by Ahmadi et al. [75], the BR algorithm's effectiveness reported similar success in predicting nanofluid viscosity using BR-trained ANNs.

The ANN model trained with the Bayesian Regularization (trainbr) algorithm all datasets consistently showed regression coefficients higher than 0.999 results as presented in Table 2 (training, testing and validation). Specifically, its exceptional R-value significantly outperforms the best results from the literature for similar predictions on nanofluid properties [78]. The ANN model is able to account for more than 99.9% of the variance in experimental thermal conductivity data, as indicated by a correlation coefficient approaching unity, highlighting the excellent predictive performance. Some reasons behind this accuracy rate may be the distinguishing superiority of BR-trained (trainbr algorithm) ANN. The Bayesian nature of the algorithm places prior information on mass and bias distributions, which helps calculate better parameter estimates [70]. Second, automatically adjusting a good number of parameters leads to intrinsic regularization (avoiding overfitting), an issue prevalent in tasks with complex modelling [84]. Finally, the robustness to noisy data and initial network conditions makes the BR method particularly useful for nanofluid property prediction where there are uncertainties in experimental data [32].

An ANN model's error distribution and predictive accuracy, trained using the trainbr function, were evaluated to assess its performance in predicting the thermal conductivity of the EG/W-based GNP/CNC hybrid nanofluid. Figure 14a presents the error histogram for a selected checkpoint during the model training process. The distribution exhibits a pronounced central peak around zero error (denoted by the

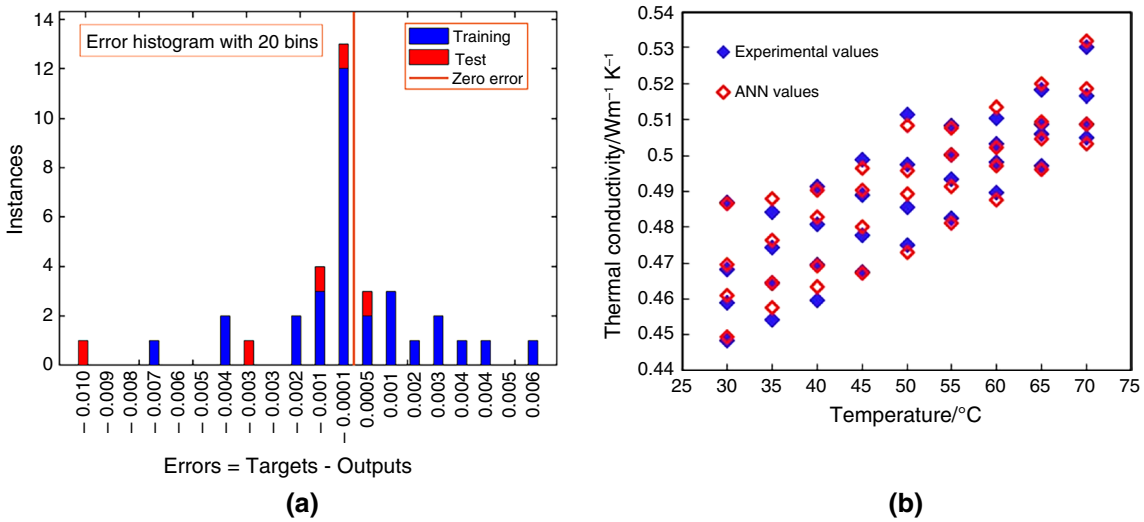

Fig. 14 **a** Error histogram **b** Comparison of experimental and ANN model data

brown line), with most samples clustered tightly around this point. This error profile is indicative of a well-calibrated model with high predictive accuracy. The symmetric and leptokurtic nature of the distribution suggests that the model has effectively captured the underlying relationships in the experimental data without significant bias or systematic errors [85]. The comparative analysis between experimental measurements and ANN predictions, illustrated in Fig. 14b, further corroborates the model's predictive capabilities across the range of temperatures and volume concentrations studied. The close alignment of predicted data points with their experimental counterparts demonstrates the model's ability to generalize effectively across the parameter space. This high concordance between observed and predicted values is a hallmark of a robust and well-trained ANN model [75]. The elevated regression coefficients observed across all datasets (training, validation, and testing) provide additional quantitative evidence of the model's reliability and generalization capacity. These high R-values, consistently exceeding 0.99, indicate that the ANN model accounts for over 99% of the variance in the thermal conductivity data, surpassing the performance metrics reported in recent literature for similar nanofluid systems [78, 86]. Thus, the error histogram analysis, in addition to directly comparing the predicted and experimental values with high regression coefficients, undoubtedly validates that both achieved ANN models developed using the trainbr function are working fine. A powerful surrogate model for accurate prediction of thermal conductivity, the EG/W-based GNP/CNC hybrid nanofluid is obtained within a range of temperatures and concentrations, which can be exploited to approximate and optimize the thermal properties of the nanofluid system.

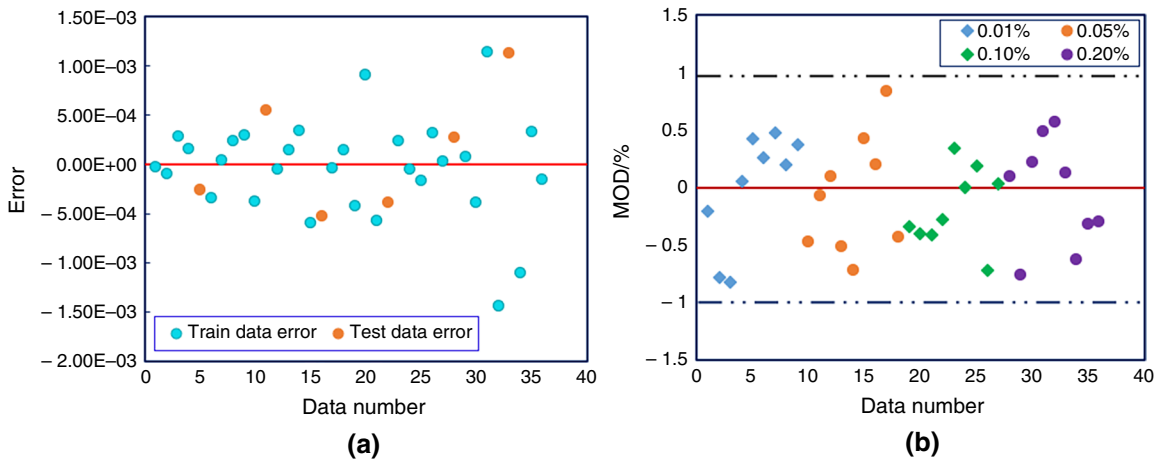

Fig. 15 **a** Error values of train data and test data. **b** Margin of deviation (MOD)

Figure 15a illustrates the error distribution for training and testing datasets. The error, defined as the difference between predicted and experimental values, is confined within a narrow range of $\pm 1 \times 10^{-3}$. This tight error band demonstrates the high precision of the ANN model in thermal conductivity prediction across varied nanofluid compositions and conditions. Figure 15b depicts the MOD as a function of nanoparticle volume concentration. The MOD, a metric quantifying the relative deviation of predicted values from experimental data, exhibits a maximum value of 1% across all concentrations studied. This consistently low MOD value underscores the model's robust predictive capability across the entire range of nanofluid compositions investigated.

The minimal error range as seen in Fig. 15a and low MOD values illustrated in Fig. (b) highlighted the accuracy and reliability of the ANN-based developed model. These results are remarkable considering nanofluid thermal conductivity's complex, nonlinear behaviour. This result was comparable to recent examples in the literature of nanofluid properties prediction with machine learning [75, 78]. This inferential probing reveals that the optimized ANN architecture and the Bayesian Regularization training algorithm theoretically apprehend complex physicochemical interactions underlying thermal conductivity in GNP/CNC hybrid nanofluid systems. The high accuracy of the model at different concentrations demonstrates its potential to be used for nanofluid design and optimization in thermal management.

Comparative analysis of ANN models

In recent years, the property prediction of nanofluids has improved due to ANN models being one of the most influential tools for predictive modelling in complex colloidal systems. This work compares ANN models against recently developed methods, critically analysing the progress made by other works. The comparison considers different ANN structures, training algorithms, and performance measures to provide a complete overview of various nanofluid modelling approaches under development. Kishore et al. [87] set an early milestone in this line through their ANN model of ternary nanofluids. They used a 7–9-2 network with the Levenberg–Marquardt (LM) algorithm, obtaining a Mean Squared Error of 5.7×10^{-4} and correlation coefficient $R = 0.99496$. This laid the foundation for future work in multi-component nanofluid property prediction and highlighted that ANNs had scope to model complex fluid behaviours. Hybrid nanofluids have specifically been used in several studies, each taking advantage of different issues brought about by these new types of materials. Another significant effort by researchers used the Group Method of Data Handling (GMDH)-ANN [88] to reduce the RMSE further and achieve $R = 0.994$, MSE = 0.0013 with acceptable implementation in multi-objective optimization. This study illustrated the advantage of robust ANN architectures in dealing with complex, nonlinear chemical behaviours in hybrid nanofluid systems. This was followed by more refined techniques thanks to additional developments. An artificial intelligence model, based on appearance [89], is able to predict relative and absolute viscosity ($R = 0.99$; Mean Absolute Percentage Error: MAPE = 0.3100). This work showed the capability of AI techniques other than conventional ANN applications for characterizing nanofluids. Moreover, a Least Mean Square-Backpropagation Neural Network (LMS-BPNN) [90] employed on ternary hybrid nanofluids produced an inadequate error of about 10^{-6}, which shows the efficiency of hybrid training algorithms in enhancement prediction accuracy.

Recent contributions studied different ANN architectures to improve performance. It was reported in [91] that a thermal conductivity prediction with $R = 0.9947$ and MSE = 3.5291×10^{-7} was obtained using one hidden layer ANN for determining the nanofluid characteristics, indicating the capacity of simple network configurations to extract nanofluid features. On the contrary, ANN was established for the two-hidden layer to predict thermal conductivity and viscosity using a 2–5–7–1 network structure reported $R = 0.999$ with MSE (coefficient values of at most $\times -10^{-6}$) [91]. This study indicated the benefits of utilizing deeper network architectures to predict these two output parameters together. Regarding this component, our proposed ANN model is unique in several aspects. Our trained models use a 2–10–1 architecture that is optimized to provide the best balance between complexity and generalization. After comprehensive comparisons with 15 other training algorithms, the Levenberg–Marquardt algorithm was chosen for its best convergence and stability. As the nanoparticles used in nanofluids are large, their behaviour is complex and not regular; our model employs a tan-sigmoid activation function as an ANN classifier for the nonlinear mapping ability of GNPs/CNC hybrid nanofluid.

The most outstanding is the performance of our model, with a coefficient correlation equal to 0.9999 and an MSE of 4.8352×10^{-7}. A 27.1% MSE reduction compared to the next best-performing model in the literature [92] and a better R-value. It is even more substantial considering the difficulty in predicting the thermal conductivity of GNPs/CNC hybrid nanofluids and their specific highly complex, nonlinear character. The factors contributing to our model's striking performance are multi-fold due to consideration for network architecture optimization; appropriate training algorithm selection and through dataset curation and pre-processing are apparent. These components coalesce to deliver a strong signal that can generate much faster and more accurate predictions than existing models. These other works show that increasingly complex ANN architectures and hybrid training

Table 8 Comparison of the proposed model with different published methods based on their respective network structures, training algorithms, activation functions, input/output parameters, and accuracy metrics

Refs.	Method	Structure	TA/AF	Input/output	Accuracy
[87]	ANN	7–9–2	LM/Sigmoid, purelin	T, φ, water, Al_2O_3, EG, G, CuO/k_{nf},μ_{nf}	MSE = 0.00057 R = 0.99496
[91]	ANN	2–15–1	LM-BP	φ, T/k_{nf}	R = 0.9947, MSE = 3.529×10^{-7}
[92]	ANN	2–5–7–1	LM Tansig, Logsign, purelin	φ, T/k_{nf}	R = 0.999, MSE = 6.333×10^{-6}
[93]	ANN	2–3–2	LM/Tangent sigmoid	φ, T/k_{nf},μ_{nf}	MSE = 4.51×10^{-06} R = 0.9896
[94]	ANN	8–10–2	LM/Sigmoid, purelin	Cp_{bf}, ρ_p, k_{bf}, d_p, φ, μ_{bf}, k_p, ρ_{bf}/k_{nf},μ_{nf}	MSE = 0.001133
[95]	ANN	3–6–10–1	SGD/ReLU, Tanh	φ, T, d_p/k_{nf},μ_{nf}	R = 0.9974, MSE = 5.5044×10^{-4}
Our study	ANN	2–10–1	LM/Tansig, purelin	φ, T/k_{nf},	R = 0.999, MSE = 4.8352×10^{-7}

T = temperature, φ = Volume concentration, k_{nf} = Thermal conductivity of nanofluid, μ_{nf} = Viscosity of nanofluid, Cp_{bf} = Specific heat capacity of base fluid, ρ_p = Density of nanoparticles, k_{bf} = Thermal conductivity of basefluid, d_p = Particle size, φ = Particle volume fraction, μ_{bf} = Viscosity of basefluid, k_p = Thermal conductivity of nanoparticles, ρ_{bf} = Density of basefluid

algorithms are applied to nanofluid property prediction. Nevertheless, our results show that single hidden layer networks tuned properly can even outperform more complex systems in some instances, illustrating the need for specific model design with a particular nanofluid system.

Table 8 compares the proposed model with different published methods based on their respective network structures, training algorithms, activation functions, input/output parameters, and accuracy metrics. These methods' input includes nanofluid and base liquid parameters, such as temperature, volume concentration, thermal conductivities, viscosity, specific heat capacities, particle size, and density. Our proposed model also uses input/output in these seven parameters. Our neural network model provides better accuracy and performance than the previously published methods. It can accurately predict the thermophysical properties of nanofluids across various concentrations using only five or three neurons in one hidden layer. Overall, this model shows the potential of neural networks in the multi-parameter prediction required to model nanofluids. It can also incorporate domain knowledge using physics-informed neural networks that can be more accurate and interpretable than black-box artificial neural network models. Moreover, the proposed transfer learning methods can also exploit pre-trained models on different nanofluid compositions, facilitating faster material characterization.

Conclusions

The analysis of graphene nanoplatelet and cellulose nanocrystal hybrid nanofluids has led to significant advancements in nanofluid-based thermal management. The study is based on an elaborate approach that combines experimental testing and machine learning techniques, which allows the researchers to arrive at several important conclusions. For instance, the optimal level of colloidal stability was found at a concentration of 0.1% by volume of GNPs/CNC in a 60:40 ethylene glycol/water base fluid. The UV–Vis spectroscopical analysis confirmed the peak absorption at the 0.10% and 0.20% concentrations, indicating better suspension stability. Thermogravimetric analysis determined the nature of thermal degradation, with the mass reduction in the nanofluid initiated at around 130 °C and fully degraded at approximately 500 °C. The 0.20% GNP: CNC nanofluid, in turn, demonstrated a better level of thermal degradation at the outset, increasing it to 150 °C and thereby improving its suitability for applications at high temperatures. The present study has developed an ANN model for thermal conductivity prediction that is parallel to the experimental work. The optimized ANN architecture provides exceptional predictive accuracy, including a single hidden layer with ten neurons and tansig and purlin transfer functions. The Bayesian regularization backpropagation function showed the best performance, providing the coefficient of determination of 99.99%, mean squared error of 4.8352×10^{-7}, and root mean square error of 1.2083×10^{-3}. Therefore, the model can be termed valuable due to its strong predictive abilities, which can be applied to estimate nanofluid properties quickly.

The results have several implications across various significant of thermal management and nanofluid engineering. The developed optimized hybrid nanofluid. Composed of GNPs and CNC, it can be implemented as an effective solution for enhancing the efficiency of heat transfer in automotive radiators and beyond. Further, its improved thermal stability can widen the spectrum of potential applications to high-temperature industrial processes. Simultaneously, a developed ANN model demonstrates high accuracy, making it a helpful predictive tool. In this way, it could aid in accelerating the implementation of nanofluid by optimizing the processes of its design and application development. However, it is noted that this study has several limitations. The investigation was limited to volume concentrations (0.01%–0.2%), and the thermal conductivity measurements

were conducted between 30 and 80 °C. In addition, the comprehensive study as it was presented in this manuscript was carried out for a single EG: W ratio (60:40), with no further efforts undertaken to evaluate stability in the long-term (that goes beyond the capabilities of experimental duration). These limitations thus limit future research prospects. Further studies may focus on the characteristics of the nanofluid over its operational range, including at higher concentration volume fractions and beyond 80 °C. Furthermore, systematic studies of different base fluid compositions on nanofluid properties would be beneficial in formulating more optimized lubricants. Long-term stability studies are necessary, especially in determining the degradation of its performance at longer operational times. It should be noted at this point that as the results from laboratory investigations and practical implementations vary to a certain extent, in situ testing of the hybrid nanofluid in real automotive radiator systems or other heat transfer applications could fill this gap. ANN models can be further improved with more variables, such as other physicochemical parameters and advanced machine learning techniques like deep learning and ensemble methods to make accurate and robust predictions.

In conclusion, these results demonstrate a sound groundwork for preparing efficient and stable hybrid nanofluids capable of being adopted as advanced thermal management materials. It paves the way for significant improvements in heat transfer efficiency across different industries and can revolutionize thermal management solutions ranging from automotive cooling to industrial heat exchangers. The resulting nanofluid of optimized composition and this accurate predictive model represent essential engineering tools for developing and eventually deploying industrial formulations. The advances can spark the development of sustainable, efficient, next-generation thermal management technologies and place GNP-CNC hybrid nanofluids at the cutting edge of future cooling solutions.

Acknowledgements The authors express gratitude to the University Malaysia Pahang Al-Sultan Abdullah (UMPSA), Malaysia, for giving laboratory resources and financial support under the International Publication Research Grant No. RDU223301.

Author contributions Md. Munirul Hasan involved in data curation, methodology, software, original draft preparation and visualization, Md. Mustafizur Rahman took part in supervision, idea generation, conceptualization, reviewing, editing and validation; Suraya Abu Bakar involved in supervision, reviewing, and editing; Devarajan Ramasamy involved in experimental study; drafting; investigation; A H M Saifullah Sadi involved in reviewing and editing; Muhammad Nomani Kabir took part in supervision and software.

Funding The authors extend their appreciation to Universiti Malaysia Pahang Al-Sultan Abdullah, Malaysia, for their provision of laboratory facilities and financial assistance. This research has been made possible through the support of the International Publication Research Grant No. RDU223301.

Data availability Data and materials will be provided based on request.

Declarations

Conflict of interest The authors disclaim any knowledge of conflicting financial interests or personal connections that might have influenced the work presented in this publication.

Ethical approval This declaration is not applicable.

References

1. Sajid MU, Ali HM. Recent advances in application of nanofluids in heat transfer devices: a critical review. Renew Sustain Energy Rev. 2019;103:556–92.
2. Huminic G, Huminic A. Hybrid nanofluids for heat transfer applications–a state-of-the-art review. Int J Heat Mass Transf. 2018;125:82–103.
3. Sundar LS, Sharma KV, Singh MK, Sousa A. Hybrid nanofluids preparation, thermal properties, heat transfer and friction factor–a review. Renew Sustain Energy Rev. 2017;68:185–98.
4. Babar H, Ali HM. Towards hybrid nanofluids: preparation, thermophysical properties, applications, and challenges. J Mol Liq. 2019;281:598–633.
5. Vallejo JP, Prado JI, Lugo L. Hybrid or mono nanofluids for convective heat transfer applications. A critical review of experimental research. Appl Thermal Eng. 2022;203:117926.
6. Sarkar J, Ghosh P, Adil A. A review on hybrid nanofluids: recent research, development and applications. Renew Sustain Energy Rev. 2015;43:164–77.
7. Pérez Vallejo J, Iglesias Prado JI, Lugo Latas L. Hybrid or mono nanofluids for convective heat transfer applications. A critical review of experimental research. Appl Thermal Eng. 2022;203:117926.
8. Esfe MH, Arani AAA, Rezaie M, Yan W-M, Karimipour A. Experimental determination of thermal conductivity and dynamic viscosity of Ag–MgO/water hybrid nanofluid. Int Commun Heat Mass Transfer. 2015;66:189–95.
9. Arbak A, Attar A, Yapaoz MA, Armağan M, Bulbul Y, Demir EK, et al. Experimental investigation of bimetallic nanoparticles heat transfer characteristics in automotive radiators. Case Stud Thermal Eng. 2023;43: 102763.
10. Sandhya M, Ramasamy D, Kadirgama K, Harun W, Saidur R. Experimental study on properties of hybrid stable & surfactant-free nanofluids GNPs/CNCs (Graphene nanoplatelets/cellulose nanocrystal) in water/ethylene glycol mixture for heat transfer application. J Mol Liq. 2022;348: 118019.
11. Kazemi I, Sefid M, Afrand M. A novel comparative experimental study on rheological behavior of mono & hybrid nanofluids concerned graphene and silica nano-powders: characterization, stability and viscosity measurements. Powder Technol. 2020;366:216–29.
12. Eshgarf H, Kalbasi R, Maleki A, Shadloo MS, Karimipour A. A review on the properties, preparation, models and stability of hybrid nanofluids to optimize energy consumption. J Therm Anal Calorim. 2021;144:1959–83.
13. Younes H, Mao M, Murshed SS, Lou D, Hong H, Peterson G. Nanofluids: key parameters to enhance thermal conductivity and its applications. Appl Therm Eng. 2022;207: 118202.
14. Turkyilmazoglu M. Two models on the unsteady heat and fluid flow induced by stretching or shrinking sheets and novel

time-dependent solutions. ASME J Heat Mass Transf. 2024;146: 101802.
15. Elsaid K, Abdelkareem MA, Maghrabie HM, Sayed ET, Wilberforce T, Baroutaji A, et al. Thermophysical properties of graphene-based nanofluids. Int J Thermofluids. 2021;10: 100073.
16. Kargarzadeh H, Mariano M, Gopakumar D, Ahmad I, Thomas S, Dufresne A, et al. Advances in cellulose nanomaterials. Cellulose. 2018;25:2151–89.
17. Sandhya M, Ramasamy D, Sudhakar K, Kadirgama K, Samykano M, Harun W, et al. A systematic review on graphene-based nanofluids application in renewable energy systems: preparation, characterization, and thermophysical properties. Sustain Energy Technol Assess. 2021;44: 101058.
18. Wang Y, Oon CS, Foo J-J, Tran M-V, Nair SR, Low FW. Numerical investigation of thermo-hydraulic performance utilizing clove-treated graphene nanoplatelets nanofluid in an annular passage with perforated curve fins. Results Eng. 2023;17: 100848.
19. Tiong ACY, Tan IS, Foo HCY, Lam MK, Mahmud HB, Lee KT, et al. Study on the synergism of cellulose nanocrystals and janus graphene oxide for enhanced oil recovery. Geoenergy Sci Eng. 2023;221: 111242.
20. Habibi Y, Lucia LA, Rojas OJ. Cellulose nanocrystals: chemistry, self-assembly, and applications. Chem Rev. 2010;110:3479–500.
21. Akilu S, Sharma K, Baheta AT, Mamat R. A review of thermophysical properties of water based composite nanofluids. Renew Sustain Energy Rev. 2016;66:654–78.
22. Kim HJ, Jeong JH, Choi YH, Eom Y. Review on cellulose nanocrystal-reinforced polymer nanocomposites: Processing, properties, and rheology. Korea-Australia Rheol J. 2021;33(3):165–85.
23. Xu X, Liu F, Jiang L, Zhu J, Haagenson D, Wiesenborn DP. Cellulose nanocrystals vs. cellulose nanofibrils: a comparative study on their microstructures and effects as polymer reinforcing agents. ACS Appl Mater Interfaces. 2013;5(8):2999–3009.
24. Yaw CT, Koh S, Sandhya M, Kadirgama K, Tiong SK, Ramasamy D, et al. Heat transfer enhancement by hybrid nano additives—graphene nanoplatelets/cellulose nanocrystal for the automobile cooling system (radiator). Nanomaterials. 2023;13:808.
25. Sandhya M, Ramasamy D, Kadirgama K, Harun W, Saidur R. Assessment of thermophysical properties of hybrid nanoparticles [Graphene Nanoplatelets (GNPs) and cellulose nanocrystal (CNC)] in a base fluid for heat transfer applications. Int J Thermophys. 2023;44:55.
26. Basu A, Saha A, Banerjee S, Roy PC, Kundu B. A review of artificial intelligence methods in predicting thermophysical properties of nanofluids for heat transfer applications. Energies. 2024;17:1351.
27. Esfe MH, Amoozadkhalili F, Toghraie D. Determining the optimal structure for accurate estimation of the dynamic viscosity of oil-based hybrid nanofluid containing MgO and MWCNTs nanoparticles using multilayer perceptron neural networks with Levenberg-Marquardt Algorithm. Powder Technol. 2023;415: 118085.
28. Khandokar I, Hasan M, Ernawan F, Islam S, Kabir MN. Handwritten character recognition using convolutional neural network. J Phys Conf Ser. 2021;1918: 042152.
29. Afrand M, Najafabadi KN, Akbari M. Effects of temperature and solid volume fraction on viscosity of SiO2-MWCNTs/SAE40 hybrid nanofluid as a coolant and lubricant in heat engines. Appl Therm Eng. 2016;102:45–54.
30. Li X, Zou C, Wang T, Lei X. Rheological behavior of ethylene glycol-based SiC nanofluids. Int J Heat Mass Transf. 2015;84:925–30.
31. Rostami S, Toghraie D, Shabani B, Sina N, Barnoon P. Measurement of the thermal conductivity of MWCNT-CuO/water hybrid nanofluid using artificial neural networks (ANNs). J Therm Anal Calorim. 2021;143:1097–105.
32. Esfe MH, Ahangar MRH, Rejvani M, Toghraie D, Hajmohammad MH. Designing an artificial neural network to predict dynamic viscosity of aqueous nanofluid of TiO2 using experimental data. Int Commun Heat Mass Transfer. 2016;75:192–6.
33. Aa A, Mohammed KJ, Smaisim GF, Hadrawi SK, Zekri H, Andani HT, et al. Evaluation of the effects of the presence of ZnO-TiO2 (50%–50%) on the thermal conductivity of Ethylene Glycol base fluid and its estimation using Artificial Neural Network for industrial and commercial applications. J Saudi Chem Soc. 2023;27: 101613.
34. Tian S, Arshad NI, Toghraie D, Eftekhari SA, Hekmatifar M. Using perceptron feed-forward Artificial Neural Network (ANN) for predicting the thermal conductivity of graphene oxide-Al2O3/water-ethylene glycol hybrid nanofluid. Case Stud Thermal Eng. 2021;26: 101055.
35. Esfe MH, Esfandeh S, Toghraie D. Investigation of different training function efficiency in modeling thermal conductivity of TiO2/Water nanofluid using artificial neural network. Colloids Surf A. 2022;653: 129811.
36. Foresee FD, Hagan MT, editors. Gauss-Newton approximation to Bayesian learning. In: Proceedings of international conference on neural networks (ICNN'97); 1997: IEEE.
37. Hanin B, Zlokapa A. Bayesian interpolation with deep linear networks. Proc Natl Acad Sci. 2023;120:2301345120.
38. Ajuka LO, Odunfa MK, Oyewola MO, Ikumapayi OM, Akinlabi SA, Akinlabi ET. Modeling of viscosity of composite of TiO2–Al2O3 and ethylene glycol nanofluid by artificial neural network: experimental correlation. IJIDeM. 2024;18:1969–78.
39. Esfe MH, Raki HR, Emami MRS, Afrand M. Viscosity and rheological properties of antifreeze based nanofluid containing hybrid nano-powders of MWCNTs and TiO2 under different temperature conditions. Powder Technol. 2019;342:808–16.
40. Bakhtiari R, Kamkari B, Afrand M, Abdollahi A. Preparation of stable TiO2-Graphene/Water hybrid nanofluids and development of a new correlation for thermal conductivity. Powder Technol. 2021;385:466–77.
41. Sandhya M, Ramasamy D, Sudhakar K, Kadirgama K, Harun W. Ultrasonication an intensifying tool for preparation of stable nanofluids and study the time influence on distinct properties of graphene nanofluids–a systematic overview. Ultrason Sonochem. 2021;73: 105479.
42. Hussein AM, Sharma K, Bakar R, Kadirgama K. The effect of nanofluid volume concentration on heat transfer and friction factor inside a horizontal tube. J Nanomater. 2013;2013: 859563.
43. Urmi WT, Rahman M, Kadirgama K, Ramasamy D, Maleque M. An overview on synthesis, stability, opportunities and challenges of nanofluids. Mater Today Proc. 2021;41:30–7.
44. Safiei W, Rahman M, Yusoff A, Radin M. Preparation, stability and wettability of nanofluid: a review. J Mech Eng Sci. 2020;14:7244–57.
45. Benedict F, Kumar A, Kadirgama K, Mohammed HA, Ramasamy D, Samykano M, et al. Thermal performance of hybrid-inspired coolant for radiator application. Nanomaterials. 2020;10:1100.
46. Tantra R, Schulze P, Quincey P. Effect of nanoparticle concentration on zeta-potential measurement results and reproducibility. Particuology. 2010;8:279–85.
47. Dukhin SS, Kretzschmar G, Miller R. Dynamics of adsorption at liquid interfaces: theory, experiment, application. Amsterdam: Elsevier; 1995.
48. Sennett P, Olivier J. Colloidal dispersions, electrokinetic effects, and the concept of zeta potential. Ind Eng Chem. 1965;57:32–50.
49. Saoudi L, Girard HA, Larquet E, Mermoux M, Leroy J, Arnault J-C. Colloidal stability over months of highly crystalline

high-pressure high-temperature hydrogenated nanodiamonds in water. Carbon. 2023;202:438–49.
50. Urmi WT, Rahman M, Kadirgama K, Ramasamy D. Exploring surfactant-enhanced stability and thermophysical characteristics of water-ethylene glycol-based Al2O3-TiO2 hybrid nanofluids. WSEAS Trans Heat Mass Transf. 2023;18:195–206.
51. Borode A, Tshephe T, Olubambi P, Sharifpur M, Meyer J. Stability and thermophysical properties of GNP-Fe2O3 hybrid nanofluid: effect of volume fraction and temperature. Nanomaterials. 2023;13:1238.
52. Gul T, Nasir S, Berrouk AS, Raizah Z, Alghamdi W, Ali I, et al. Simulation of the water-based hybrid nanofluids flow through a porous cavity for the applications of the heat transfer. Sci Rep. 2023;13:7009.
53. Lin H, Jian Q, Bai X, Li D, Huang Z, Huang W, et al. Recent advances in thermal conductivity and thermal applications of graphene and its derivatives nanofluids. Appl Therm Eng. 2023;218: 119176.
54. Asadi A, Pourfattah F, Szilágyi IM, Afrand M, Żyła G, Ahn HS, et al. Effect of sonication characteristics on stability, thermophysical properties, and heat transfer of nanofluids: a comprehensive review. Ultrason Sonochem. 2019;58: 104701.
55. Nagarajan K, Ramanujam N, Sanjay M, Siengchin S, Surya Rajan B, Sathick Basha K, et al. A comprehensive review on cellulose nanocrystals and cellulose nanofibers: Pretreatment, preparation, and characterization. Polym Compos. 2021;42(4):1588–630.
56. Ali HM. Advances in Nanofluid Heat Transfer. Amsterdam: Elsevier; 2022.
57. Edition I. ASHRAE Handbook-Fundamentals. SI. Am Soc Heating, Refrig Air-Conditioning Eng Inc; 2009.
58. Asadi A, Asadi M, Rezaniakolaei A, Rosendahl LA, Afrand M, Wongwises S. Heat transfer efficiency of Al2O3-MWCNT/thermal oil hybrid nanofluid as a cooling fluid in thermal and energy management applications: an experimental and theoretical investigation. Int J Heat Mass Transf. 2018;117:474–86.
59. Madkhali HA, Ahmed M, Nawaz M, Alharbi SO, Alqahtani A, Malik M. Computational study on the effects of Brownian motion and thermophoresis on thermal performance of cross fluid with nanoparticles in the presence of Ohmic and viscous dissipation in chemically reacting regime. Comput Particle Mech. 2024;11:1301–11.
60. Jang SP, Choi SU. Role of Brownian motion in the enhanced thermal conductivity of nanofluids. Appl Phys Lett. 2004;84:4316–8.
61. Alade IO, Rahman MAA, Hassan A, Saleh TA. Modeling the viscosity of nanofluids using artificial neural network and Bayesian support vector regression. J Appl Phys. 2020;128: 085306.
62. Sabir Z, Akkurt N, Said SB. A novel radial basis Bayesian regularization deep neural network for the Maxwell nanofluid applied on the Buongiorno model. Arab J Chem. 2023;16: 104706.
63. Esfe MH, Wongwises S, Naderi A, Asadi A, Safaei MR, Rostamian H, et al. Thermal conductivity of Cu/TiO2–water/EG hybrid nanofluid: experimental data and modeling using artificial neural network and correlation. Int Commun Heat Mass Transfer. 2015;66:100–4.
64. Soltani O, Akbari M. Effects of temperature and particles concentration on the dynamic viscosity of MgO-MWCNT/ethylene glycol hybrid nanofluid: experimental study. Physica E. 2016;84:564–70.
65. Møller MF. A scaled conjugate gradient algorithm for fast supervised learning. Neural Netw. 1993;6:525–33.
66. Ruder S. An overview of gradient descent optimization algorithms. arXiv preprint arXiv:1609.04747. 2016.
67. Bahiraei M, Heshmatian S. Graphene family nanofluids: a critical review and future research directions. Energy Convers Manag. 2019;196:1222–56.
68. Ansari H, Zarei M, Sabbaghi S, Keshavarz P. A new comprehensive model for relative viscosity of various nanofluids using feed-forward back-propagation MLP neural networks. Int Commun Heat Mass Transfer. 2018;91:158–64.
69. Raissi M, Perdikaris P, Karniadakis GE. Physics-informed neural networks: A deep learning framework for solving forward and inverse problems involving nonlinear partial differential equations. J Comput Phys. 2019;378:686–707.
70. Burden F, Winkler D. Bayesian regularization of neural networks. In: Artificial neural networks: methods and applications. 2009:23–42.
71. Hemmat Esfe M, Rostamian H, Toghraie D, Yan W-M. Using artificial neural network to predict thermal conductivity of ethylene glycol with alumina nanoparticle: effects of temperature and solid volume fraction. J Therm Anal Calorim. 2016;126:643–8.
72. Jahed Armaghani D, Hasanipanah M, Mahdiyar A, Abd Majid MZ, Bakhshandeh Amnieh H, Tahir MM. Airblast prediction through a hybrid genetic algorithm-ANN model. Neural Comput Appl. 2018;29:619–29.
73. Yaw CT, Koh SP, Sandhya M, Ramasamy D, Kadirgama K, Benedict F, et al. An approach for the optimization of thermal conductivity and viscosity of hybrid (graphene nanoplatelets, GNPs: cellulose nanocrystal, CNC) nanofluids using response surface methodology (RSM). Nanomaterials. 2023;13:1596.
74. Willmott CJ, Matsuura K. Advantages of the mean absolute error (MAE) over the root mean square error (RMSE) in assessing average model performance. Climate Res. 2005;30:79–82.
75. Ahmadi MH, Nazari MA, Ghasempour R, Madah H, Shafii MB, Ahmadi MA. Thermal conductivity ratio prediction of Al2O3/water nanofluid by applying connectionist methods. Colloids Surf A. 2018;541:154–64.
76. Bahiraei M, Rahmani R, Yaghoobi A, Khodabandeh E, Mashayekhi R, Amani M. Recent research contributions concerning use of nanofluids in heat exchangers: a critical review. Appl Therm Eng. 2018;133:137–59.
77. Mahian O, Kolsi L, Amani M, Estellé P, Ahmadi G, Kleinstreuer C, et al. Recent advances in modeling and simulation of nanofluid flows-Part I: fundamentals and theory. Phys Rep. 2019;790:1–48.
78. Esfe MH, Yan W-M, Afrand M, Sarraf M, Toghraie D, Dahari M. Estimation of thermal conductivity of Al_2O_3/water (40%)–ethylene glycol (60%) by artificial neural network and correlation using experimental data. Int Commun Heat Mass Transfer. 2016;74:125–8.
79. Kayri M. Predictive abilities of Bayesian regularization and Levenberg–Marquardt algorithms in artificial neural networks: a comparative empirical study on social data. Math Comput Appl. 2016;21:20.
80. MacKay DJ. Bayesian interpolation. Neural Comput. 1992;4:415–47.
81. Yaragalla S, Bhavitha KB, Athanassiou A. A review on graphene based materials and their antimicrobial properties. Coatings. 2021;11:1197.
82. Said Z, Sohail MA. Introduction to hybrid nanofluids. Hybrid nanofluids. Elsevier; 2022. p. 1–32.
83. Mohanraj M, Jayaraj S, Muraleedharan C. Applications of artificial neural networks for thermal analysis of heat exchangers–a review. Int J Therm Sci. 2015;90:150–72.
84. Oliver N. Nonlinear system identification: from classical approaches to neural networks and fuzzy models. Ch. 2001;11:294–6.
85. Willmott CJ, Robeson SM, Matsuura K. A refined index of model performance. Int J Climatol. 2012;32:2088–94.

86. Ariana M, Vaferi B, Karimi G. Prediction of thermal conductivity of alumina water-based nanofluids by artificial neural networks. Powder Technol. 2015;278:1–10.
87. Pvr NK, Venkatachalapathy S, Kalidoss P, Chaupal P. Experimental investigation with ANN modeling of thermal conductivity and viscosity of a ternary nanofluid at different mixing ratios and volume concentrations. J Mol Liquids. 2023;383: 122006.
88. Baghoolizadeh M, Jasim DJ, Sajadi SM, Rostamzadeh-Renani R, Rostamzadeh-Renani M, Hekmatifar M. Using of artificial neural networks and different evolutionary algorithms to predict the viscosity and thermal conductivity of silica-alumina-MWCN/water nanofluid. Heliyon. 2024;10:26279.
89. Borode A, Olubambi P. Optimisation of artificial intelligence models and response surface methodology for predicting viscosity and relative viscosity of GNP-alumina hybrid nanofluid: incorporating the effects of mixing ratio and temperature. J Supercomput. 2024;80:4841–69.
90. Zeeshan A, Khan MI, Ellahi R, Marin M. Computational intelligence approach for optimising MHD Casson ternary hybrid nanofluid over the shrinking sheet with the effects of radiation. Appl Sci. 2023;13:9510.
91. Çolak AB, Bayrak M. Comparison of experimental thermal conductivity of water-based Al2O3–Cu hybrid nanofluid with theoretical models and artificial neural network output. J Thermal Anal Calorim. 2024:1–16.
92. Esfe MH, Amoozad F, Hatami H, Toghraie D. Comprehensive study and scientific process to increase the accuracy in estimating the thermal conductivity of nanofluids containing SWCNTs and CuO nanoparticles using an artificial neural network. Micro Nano Syst Lett. 2024;12:5.
93. Sahin F, Genc O, Gökcek M, Çolak AB. From experimental data to predictions: artificial intelligence supported new mathematical approaches for estimating thermal conductivity, viscosity and zeta potential in Fe3O4-water magnetic nanofluids. Powder Technol. 2023;430: 118974.
94. Onyiriuka EJ. Single phase nanofluid thermal conductivity and viscosity prediction using neural networks and its application in a heated pipe of a circular cross section. Heat Transfer. 2023;52:3516–37.
95. Zhu T, Mei X, Zhang J, Li C. Prediction of thermal conductivity of EG–Al2O3 nanofluids using six supervised machine learning models. Appl Sci. 2024;14:6264.